University of Alberta

Biogeochemical Stabilization of Mercury in Contaminated Soils

By

Allison Rebecca McLean

A thesis submitted to the Faculty of Graduate Studies and Research in partial fulfillment of the requirements for the degree of Master of Science

in

Soil Science

Department of Renewable Resources

Edmonton, Alberta

Spring 2004.

Library and Archives Canada

Published Heritage Branch

395 Wellington Street
Ottawa ON K1A 0N4
Canada

Bibliothèque et Archives Canada

Direction du Patrimoine de l'édition

395, rue Wellington
Ottawa ON K1A 0N4
Canada

Your file Votre référence
ISBN: 0-612-96520-1
Our file Notre référence
ISBN: 0-612-96520-1

The author has granted a non-exclusive license allowing the Library and Archives Canada to reproduce, loan, distribute or sell copies of this thesis in microform, paper or electronic formats.

The author retains ownership of the copyright in this thesis. Neither the thesis nor substantial extracts from it may be printed or otherwise reproduced without the author's permission.

L'auteur a accordé une licence non exclusive permettant à la Bibliothèque et Archives Canada de reproduire, prêter, distribuer ou vendre des copies de cette thèse sous la forme de microfiche/film, de reproduction sur papier ou sur format électronique.

L'auteur conserve la propriété du droit d'auteur qui protège cette thèse. Ni la thèse ni des extraits substantiels de celle-ci ne doivent être imprimés ou aturement reproduits sans son autorisation.

In compliance with the Canadian Privacy Act some supporting forms may have been removed from this thesis.

While these forms may be included in the document page count, their removal does not represent any loss of content from the thesis.

Conformément à la loi canadienne sur la protection de la vie privée, quelques formulaires secondaires ont été enlevés de cette thèse.

Bien que ces formulaires aient inclus dans la pagination, il n'y aura aucun contenu manquant.

Canada

Abstract

Industrial activity in Alberta has resulted in areas contaminated by elemental mercury. A technique is needed to remediate these contaminated sites or to at least curtail the movement of mercury into other environmental regions. Conversion and precipitation of mercury as a sulphide appears an ideal method to immobilize mercury in contaminated soils due to the highly recalcitrant nature of mercury sulphide.

Mercury contaminated soils were amended with sulphate and a carbon substrate and held anaerobic for 1 to 36 weeks. Soil samples were analyzed for mercury sulphide formation after incubation. Although mercury sulphide concentrations increased by significantly throughout incubation, mercury sulphide concentrations remained below 11% of total mercury. The majority of soil mercury was organic matter bound before incubation and remained so after incubation. It appears that organic matter bound mercury is highly stable and can be considered recalcitrant.

For My Mother, Doreen C. McLean

Acknowledgments

First and foremost I would like to thank my supervisor, Dr. Marvin Dudas for giving me the opportunity to study with him. I feel it was and honour and privilege to work with you. I will remember your continual encouragement and support (especially when I wanted to quit graduate studies), and the several "pushes" to keep me moving forward in my program. Thank you.

I would also like to thank the members of my supervisory committee, Dr Salim Abboud, Dr. Phil Fedorak, and Dr. Sylvie Quideau. Each of you brought a very different point of view to my study, helping to shape and mold it into the best possible research study. Thank you for all of your help and assistance in creating this final product.

This study would not have been possible without the financial assistance of the National Science and Engineering Research Council (NSERC), the Province of Alberta and University of Alberta.

I would like to thank my many friends, family and fellow grad students who supported me throughout my graduate program. In particular I would like to thank my parents, Roy and Kathleen McLean, my husband Jonah Keim, and my dearest friend Heather Lowen. Thank you for providing a shoulder to cry on when times were tough and rejoicing with me in my successes (even though most of you had no understanding of what I was talking about)! I also cannot forget my dog, Dozer, who faithfully lay at my feet everyday that I worked on my thesis.

I would also like to thank Dr. Bill McGill for his help in the preliminary stages of this program. Your advice has been invaluable in the designing of this experiment, in particular the incubation. Thank you to Dr. Jim Robertson – aka "JR". You were always there to encourage me and to listen when I needed to talk about the joys and frustrations of being a graduate student. I will truly miss you.

Finally I would like to thank my Mother, Doreen McLean, who was not able to see me through grad school, but wanted this for me before I knew I wanted it. I love you, thank you and this one's for you!

Table of Contents

1.0 INTRODUCTION AND LITERATURE REVIEW 6

1.1 Introduction 6
1.2 Sources of Soil Mercury 6
1.3 Dynamics of Soil Mercury 7
1.3.1 Volatilization of Soil Mercury 8
1.3.2 Water Phase Mercury 8
1.3.3 Adsorption to Minerals 9
1.3.3.1 Clay Component 10
1.3.3.2 Eh and pH 10
1.3.3.3 Chemical Form 11
1.3.4 Organic Matter Bound Mercury 11
1.3.5 Organic Mercury 13
1.3.6 Mercury Sulfur Complexes 14
1.4 Conversion to Mercury Sulfide as a Remediation Technology 15
1.4.1 Dynamics of Mercury Sulfide Formation 15
1.4.2 Benefits of Mercury Sulfide Formation 18
1.5 Purpose of Study 18

2.0 MATERIALS AND METHODS 20

2.1 Soil Samples 20
2.2 Routine Characterization 20
2.3 Most Probable Number (MPN) Analysis 22
2.4 Mercury Analysis 23
2.4.1 Total Mercury in Sediments 23
2.4.2 Total Mercury in Waters 23
2.5 Microcosm Incubation 24
2.5.1 Control Microcosms 25
2.5.2 Experimental Microcosms 25
2.6 Mercury Sulfide Extraction 25
2.7 Sequential Extraction 26
2.8 Total Soluble Iron and Total Soluble Manganese Analysis 27
2.9 Precipitate Analysis 28
2.10 Gas Analysis 28

3.0 RESULTS AND DISCUSSION 29

3.1 Soil Characteristics 29
3.2 Initial Soil Mercury Distribution 30
3.3 MPN Analysis 34
3.4 Microcosm Chemistry 35
3.4.1 Redox Potential 35
3.4.2 Electrical Conductivity 38

3.4.3 pH 41
3.4.4 Sulfate Concentrations 42
3.4.5 Bicarbonate Concentrations 47
3.4.6 Total Soluble Iron 52
3.4.7 Total Soluble Manganese 56
3.4.8 Methane Analysis 60
3.5 Microcosm Mercury 61
3.5.1 Total Mercury 61
3.5.2 Nitric Acid Extractable Mercury 63
3.5.3 Mercury Sulfide 67

4.0 SUMMARY AND IMPLICATIONS 72

4.1 Summary 72
4.2 Implications 73

5.0 REFERENCES 74

APPENDIX 1 81

APPENDIX 2 82

APPENDIX 3 83

List of Tables

Table 1.1: Stability constants of Hg-S complexes 15

Table 1.2: Heats of Formation of HgS 16

Table 1.3: Ksp Values of HgS 18

Table 1.4: Removal of Hg^{2+} from Solution by SRB 18

Table 2.1: Mercury Concentrations from Soil Samples Obtained from the Turner Valley Gas Plant 20

Table 3.1: Pore water chemistry for the experimental soil. 29

Table 3.2: Results of the mercury sulfide extraction in the untreated soil. 34

Table 3.3: Numbers of acetate-utilizing SRB in the soil throughout incubation. 34

Table 3.4: Change in mercury sulfide concentration throughout the 36 wk incubation... 71

List of Figures

Figure 3.1: Distribution of mercury with particle size 31

Figure 3.2: Initial forms of mercury in the untreated soil..... 33

Figure 3.3: Photograph of a microcosm immediately after set-up..... 35

Figure 3.4: Redox potential of experimental microcosms throughout incubation..... 37

Figure 3.5: Redox potential of control microcosms throughout incubation. 37

Figure 3.6: Photograph of the black precipitate on the walls of an experimental microcosm..... 38

Figure 3.7: Photograph of the black precipitate after 24 hours of exposure to air resulting in a colour change from black to rust..... 38

Figure 3.8: Electrical conductivity of experimental microcosms throughout incubation. 40

Figure 3.9: Electrical conductivity of control microcosms throughout incubation. 40

Figure 3.10: pH of experimental microcosms throughout incubation. 42

Figure 3.11: pH of control microcosms throughout incubation..... 42

Figure 3.12: Sulfate concentrations of experimental microcosms throughout incubation. 46

Figure 3.13: Sulfate concentrations of control microcosms throughout incubation..... 46

Figure 3.14: SEM compositional analysis of black precipitate at wk 21..... 47

Figure 3.15: Bicarbonate concentrations of experimental microcosms throughout incubation..... 49

Figure 3.16: Mean bicarbonate and sulfate concentrations of experimental microcosms throughout incubation. 50

Figure 3.17: Bicarbonate concentrations of control microcosms throughout incubation. 51

Figure 3.18: Mean bicarbonate and sulfate concentrations of control microcosms throughout incubation. 51

Figure 3.19: Total soluble iron concentrations of experimental microcosms throughout incubation..... 54

Figure 3.20: Mean total soluble iron and sulfate concentrations of experimental microcosms throughout incubation. 54

Figure 3.21: SEM image of amorphous iron sulfide 55

Figure 3.22: Total soluble iron concentrations of control microcosms throughout incubation 56

Figure 3.23: Total soluble iron and sulfate concentrations of control microcosms throughout incubation. 56

Figure 3.24: Total soluble manganese concentrations of experimental microcosms throughout incubation. 58

Figure 3.25: Mean total soluble manganese and sulfate concentrations of experimental microcosms throughout incubation. 58

Figure 3.26: Total soluble manganese concentrations of control microcosms throughout incubation 59

Figure 3.27: Mean total soluble manganese and sulfate concentrations of experimental microcosms throughout incubation. 60

Figure 3.28: Total mercury concentrations in experimental microcosms throughout incubation 63

Figure 3.29: Total mercury concentrations in control microcosms throughout incubation. 63

Figure 3.30: Nitric acid extractable mercury concentrations in experimental microcosms throughout incubation. 67

Figure 3.31: Nitric acid extractable mercury concentrations in control microcosms throughout incubation. 67

Figure 3.32: Mercury sulfide concentrations in experimental microcosms throughout incubation 70

Figure 3.33: Mercury sulfide concentrations in control microcosms throughout incubation 70

Figure 3.34: Distribution of mercury throughout incubation in control and experimental microcosms. 71

1.0 Introduction and Literature Review

1.1 Introduction

Natural mercury (Hg) concentrations in soils vary depending upon the type of parent material, pH, and soil organic matter (SOM) content. Because soils and sediments are composed of particles derived from the mechanical and chemical weathering of rocks, they should have low mercury concentrations if left undisturbed by civilization (Landi and Fagioli, 1994). Mercury is naturally present in soil in concentrations ranging from a few parts per billion to a few hundred parts per billion (ppb), depending upon soil texture, organic matter content, pH, and parent geologic materials (Dudas and Pawluk, 1976). Typical, uncontaminated Alberta soils range from 18 ppb to 146 ppb (Dudas and Pawluk, 1976). Naturally high concentrations of mercury, 1 to 10 parts per million (ppm), are associated with cinnabar or mercury sulfide (HgS) deposits (Adriano, 1986).

Mercury contaminated soils and sediments represent a serious potential risk to the environment and human health (Revis et al., 1989a). One of the primary terrestrial exposure pathways suspected of contributing to high mercury concentrations in humans is the incidental ingestion of contaminated soils (Davis et al., 1997). Growing public awareness of the dangers of mercury poisoning has created demands for remediation techniques with increased efficiency and removal of mercury from soil systems.

1.2 Sources of Soil Mercury

Throughout history mercury contamination of the environment has been a serious problem. The problem is not entirely with its use, but with its escape into the environment, where it can potentially end up in soils and sediment. Direct mercury contamination of soils can occur through industrial uses and waste disposal (Stewart and

Bettany, 1982). One area of particular concern regarding mercury contamination is the natural gas industry. Mercury contamination is a common, yet serious problem associated with former gas plant sites, wellhead, metering sites, pipelines, gas transmission lines, and underground storage facilities (Wren and Farrell, 1995). This is mainly due to the use of manometers, instruments using mercury to measure gas pressure. Each manometer typically contains 3 to 5 kg of mercury (Harju et al., 1995). During the operation of these sites, manometers were broken and elemental liquid phase mercury was subsequently released into the environment. Upon the decommissioning and closure of these plants and monitoring sites the mercury problem was usually left in place. Within Alberta alone, there are hundreds of these sites, thus the potential for mercury contamination is enormous.

1.3 Dynamics of Soil Mercury

Naturally, mercury occurs as cinnabar (αHgS) or meta-cinnabar (βHgS), an insoluble HgS ore (Ehrlich, 1981). Mercury sulfide ore is found as a primary mineral in igneous rocks. It can also occur as a secondary mineral in sedimentary rocks, however it is not uniformly distributed; instead it is concentrated in regions generally associated with shale and other sedimentary deposits (Jonasson and Boyle, 1971).

Under normal conditions of temperature and pressure occurring within the soil environment, mercury may be present in three oxidation states, Hg^{o} (elemental mercury), Hg^{+} (mercurous ion), and Hg^{2+} (mercuric ion) (Renneberg, 2000). Hg^{o} and Hg^{+} are unstable within the soil environment and tend to transform towards more stable products (Anderson, 1979). More than 98% of soil mercury is found as nonalkyl Hg(II) compounds and complexes (Davis et al., 1997). Mercury found in soils can be:

volatilized, dissolved (free ion complex), adsorbed to soil minerals, chelated (bound to organic matter), in organic forms, and as sulfur complexes (Schuster, 1991). Speciation of mercury is dependent upon the nature of the release, its physical and chemical properties, and the chemistry of the receiving soil (Davis et al., 1997). Of total mercury present in soil, approximately 90% is inorganic, 0.01% organic, and 6% Hg^{o} (Revis et al., 1989a).

1.3.1 Volatilization of Soil Mercury

Upon initial contamination of soil by mercury, it is readily re-emitted to the atmosphere through volatilization (Lindberg et al., 1995). Rates of volatilization depend upon initial mercury concentrations, soil texture, and biological activity (Rogers and McFarlane, 1978; Lindberg et al., 1995). The rate of volatilization increases with increasing concentration of soil mercury inputs, however mercury volatilization tends to decrease in fine textured soils (Rogers and McFarlane, 1978). Biological activity has been found to have a pronounced influence on volatilization of mercury from soils. Microbes mediate reduction of Hg^{2+} to Hg^{o} therefore soils with decreased biological activity are found to have decreased rates of volatilization (Lindberg et al., 1995; Rogers and McFarlane, 1978).

1.3.2 Water Phase Mercury

Most mercury compounds are bound to soil components (mineral and organic) therefore concentrations of water phase mercury are generally quite low in soil water (Schuster, 1991; Renneberg and Dudas, 2001). The mercuric ion is stable in solution at neutral pH conditions and under acidic, reducing conditions exists as Hg_2^{2+} (Davis et al., 1997). Chloride (Cl^-) and hydroxide (OH^-) are considered two of the most mobile and

persistent complex agents for mercury (Schuster, 1991) because they can be of sufficiently high concentrations and possess large enough stability constants, thereby dominating most natural soil systems (Clever et al., 1985). In aqueous solutions where Hg^{2+} dominates and the pH is acidic to neutral complexes with Cl^- form soluble $HgCl^+$ and $HgCl_2$, and HgClOH and $Hg(OH)_2^o$ forms under neutral conditions (Davis et al., 1997; Schuster, 1991). The mercuric ion will hydrolyze in a pH range of 2 to 6, with the final species being the soluble $Hg(OH)_2$ found at a pH of 6. Precipitation of $Hg(OH)_2$ occurs only if concentrations of Hg^{2+} exceed 107 *mg kg-1* (Hahne and Kroontje, 1973).

The influence of dissolved ligands (SO_4^{2-}, CO_3^{2-}, organic acids, dissolved humic substances) within the soil solution is considerable (Lumsdon et al., 1995). These ligands react with mercury present in the soil solution and decrease its ability to sorb onto solid soil components. Under certain pH and redox conditions ligand complexes can inhibit mercury adsorption onto soil solids due to strong complex formation and possible competition between ligands and mercury for sorption sites. However, only a small change may occur in the extent of adsorption if ligands have weak complex forming abilities and exhibit a lack of affinity for soil solids.

1.3.3 Adsorption to Minerals

Adsorption and desorption of mercury with soil minerals is recognized as an important process in the fate of mercury in soil (Yin et al., 1996). Schuster (1991) states there are two ways in which mercury adsorbs to soils: specifically and non-specifically. Covalent or coordinative forces result in specific adsorption, whereas non-specific adsorption is a result of electrostatic forces. Specific adsorption of mercury onto mineral surfaces involves reactions between dissolved mercury and functional groups of solid

mineral surfaces (Schuster, 1991). Adsorption of mercury onto minerals varies with soil texture, pH, redox conditions and the chemical form of mercury present (Steinnes and Salbu, 1995; Yin et al., 1996).

1.3.3.1 Clay Component

In soils, the clay fraction dominates adsorption and desorption reactions, due to their negative charge. However, the amount of mercury adsorbed by clay minerals depends upon the mineral type present. Clay minerals are arranged in the following series according to mercury adsorption capacity: illite > montmorillonite > kaolinite (Obukhovskaya, 1982). Illite and montmorillonite are able to fix increasing amounts of mercury compared to kaolinite due to their structural makeup. Illite and montmorillonite have a 2:1 type structure, with exchange sites available both internally and externally. Kaolinite has a 1:1 type structure therefore binding occurs on external surface exchange sites only (Obukhovskaya, 1982). Due to the presence of oxide and oxyhydroxide minerals, sorption of mercury by soil minerals increases with rising pH values.

1.3.3.2 Eh and pH

Soil redox potential (Eh) plays an important role in the form of mercury present within soils and subsequent sorption processes. Eh is pH sensitive and should be measured in conjunction with pH; in general a rise in pH results in the reduction of oxidizing potential for a given reaction (Siegel, 1974). Within soils, the most soluble mercury species are found only under highly oxygenated conditions (Eh of +350 to +400mV) (Siegel, 1974), whereas the most stable and insoluble forms are found under reducing conditions.

1.3.3.3 Chemical Form

Adsorption of mercury onto soil mineral components is dependent on the chemical form of mercury ions present in the soil solution (Hogg et al., 1978) and the presence of mercury in soil solution and its ability to participate in exchange reactions. Sorption of various soluble forms of mercury can be described in terms of Langmuir isotherms, which reflect the combined influence of soil properties and chemical properties of mercury forms present (John, 1972). Kaiser and Tolg (1980) report that organic and inorganic mercury compounds (with the exception of HgS) are soluble, but Hg^{o} is relatively insoluble in aqueous solutions. Within soils the most common species of mercury present are: $HgCl_2$, HgO, HgS, Hg^{o}, and $HgCH_3Cl$. $HgCl_2$ is only weakly retained by mineral matter, and sorption by minerals is dominant in neutral to alkaline soils (Anderson, 1979). According to Willett et al. (1992), HgO does not bind to soil mineral components, therefore tending to leach immediately upon its formation, whereas HgS and Hg^{o} rarely leach out of soils. Methyl mercury chloride ($HgCH_3Cl$) readily binds to soil components, therefore it is less likely to enter solution and become susceptible to leaching (Hogg et al., 1978).

1.3.4 Organic Matter Bound Mercury

Depending upon soil organic matter content and pH, mercury can undergo chelation, ionic exchange, inner and outer-sphere complex formation, adsorption and/or co-precipitation. Up to 85% of total soil mercury is bound to soil organic matter (Renneberg and Dudas, 2001). Irrespective of pH, the affinity of humic acid for mercury is stronger than most inorganic components (Rai et al., 1984; Yin et al., 1996; Biester et al., 2002). The class B character of the chalcophile element explains the strong affinity

of mercury to sulphur containing functional groups. Soil humus contains several sulphur containing compounds and functional groups, thus explaining the affinity of mercury to SOM. Quality of SOM plays a key role in sorption processes; which is demonstrated in soils with identical mineralogy but various SOM components (Semu et al., 1986). Mercury exhibits a strong affinity for the humic acid fraction of soil humus (Schuster, 1991) due to an increased S content versus fulvic acid and humin fractions (Paul and Clark, 1996). Mercury complexes are more strongly bound to SOM compared to mineral colloids. SOM has an increased adsorption capacity, due to an increased surface area, versus mineral colloids (Yin et al., 1996). The sorption maximum of humus is correlated to surface area > organic content > cation exchange capacity > and texture (Ramamoorthy and Rust, 1976). Of the total binding sites available, 1/3 are for cation exchange and the other 2/3 for metal complexation (Schuster, 1991) therefore dissolved SOM will form stable complexes with Hg^{2+}. Yin et al. (1996) report the presence of SOM in solution inhibits adsorption of Hg^{2+} onto mineral surfaces.

Within soils, up to 80% of mercury can be found sorbed onto SOM (Dmytriv et al., 1995). These concentrations are associated with black, decaying, and undifferentiated organic material, the soil humus fraction. Once bound by organic materials, mercury is relatively stable and does not enter into the soil solution (Wallschlager et al., 1996). Adsorption rates of mercury onto soil organic materials are 10^3 to 10^5 times greater than rates of desorption (Rai et al., 1984). The diffusion of Hg^{2+} through intra-particle micropores of SOM may be the principle factor for the observed irreversibility (Yin et al., 1997). However, mobilization of mercury may occur upon the degradation of humic substances to which it is bound (Hempel et al., 1995; Wang et al., 1991). This

degradation can be abiotic (chemical and physical weathering) or biotic (microbial degradation) in nature. Mercury is bound in the solution phase to humic and fulvic acids, and shows a positive correlation to dissolved organic carbon (Hempel et al., 1995).

Under mildly acidic conditions (pH < 4.5 to 5) SOM is the only sorbent available to mercury and other cations in certain soils (Schuster, 1991), due to the presence of oxides and oxyhydroxides. Once neutral and basic pH conditions occur, clay minerals and iron oxides become more relevant in mercury sorption reactions (Anderson, 1979). Therefore soils with low SOM contents will show an increase in the mobility of mercury with a drop in pH.

1.3.5 Organic Mercury

Although less common than inorganic forms of mercury, organic mercury is found within various soil environments. There are two main types, mono-methyl and di-methyl. Both forms are commonly found in soils and neither demonstrates a strong affinity to bind with organic matter components (Lexmond et al., 1976). Both forms of organic mercury are volatile, however it is mono-methyl mercury that is soluble in water (Lexmond et al., 1976). Depending upon the soil environment (i.e. saturated versus unsaturated), soils can be either sinks or sources of methyl mercury (St. Louis et al., 1996). Methyl mercury will bioaccumulate within organisms and undergo biomagnification within the food chain (Morel et al., 1998), due to its lipophilic nature. This makes it by far the most toxic form of mercury (D'Itri, 1972; St. Louis et al., 1996).

Methylation of mercury can occur either abiotically or biotically. Abiotic methylation is due to bacterial exudates (methyl cobalamin), humic matter, or through trans-methylation by other methyl inorganics (CH_3I, $(CH_3)_xSn$, CH_3Si^-, and $(CH_3)_xPb$)

(Davis et al., 1997). Much of the methyl mercury within the soil environments is due to microbial methylation (Davis et al., 1997), which generally occurs under anaerobic conditions (St. Louis et al., 1996; Allan et al., 2001). Microbial methylation of mercury is mainly due to the reaction of Hg^{2+} with methyl cobalamin (Lexmond et al., 1976).

Anaerobic methylation may cease in the presence of sulfide. At low redox potentials (SO_4^{2-} reduction to S^{2-}), HgS will form and precipitate out of solution and stop the methylation process (Andersson, 1979; Lexmond et al., 1976; Revis et al., 1991). HgS is insoluble in water, leaving it unable to participate in chemical reactions. In the presence of oxygen two processes may occur. Firstly, demethylation may proceed and methyl mercury concentrations may decrease within soil systems (St. Louis et al., 1996). Secondly, aerobic conditions induce the conversion of various mercury species into Hg^{2+}, thus promoting micro-organisms to reduce and subsequently methylate mercury.

1.3.6 Mercury Sulfur Complexes

Mercury is a soft metal, therefore it readily reacts with soft ligands such as sulfide (Ravichandran et al., 1999) to form water soluble $HgSH^+$, $Hg(SH)_2$, HgS_2H^-, HgS_2^{2-}, or insoluble HgS (Table 1.1). Dissolved organic matter (DSOM) complexes with mercury due to S containing humic and fulvic acid fractions. The Hg-S complex formed depends upon pH and mercury and sulfide concentrations (Wang, 1995; Ravichandran, 1999; Schuster, 1991). Low pH and sulfide concentrations favour the formation of either αHgS or βHgS, while higher pH values and sulfide concentrations favour soluble complex formation (Wang, 1995).

Table 0.1: Stability constants of Hg-S complexes (Dyrssen and Wedborg, 1991; Ravichandran et al. 1999).

Form of Hg-S Complex	K_f
$HgSH^+$	10^{20}
$Hg(SH)_2$	$10^{37.72}$
HgS_2H^-	$10^{8.30}$
HgS_2^{2-}	$10^{1.0}$
HgS	$10^{-38.8}$

1.4 Conversion to Mercury Sulfide as a Remediation Technology

The need for an insitu immobilization of mercury in contaminated soils is needed to reduce environmental risks. Conversion and precipitation of mercury as HgS seems an ideal method to immobilize mercury in contaminated soils because mercury has a high affinity to S-containing compounds and HgS is insoluble (Biester and Zimmer, 1998; Dyrssen and Wedborg, 1991; Oji, 1998; Barnett el al., 1997).

1.4.1 Dynamics of Mercury Sulfide Formation

HgS is formed either abiogenically or biogenically, depending upon the sulfide source. The biochemical (1) and geochemical (2) reactions mediated by SRB (Donald and Southam, 1999) are:

$$2CH_2O + SO_4^{2-} \rightarrow H_2S + 2HCO_3^- \quad (1)$$

$$M^{2+} + H_2S \rightarrow MS_{(s)} + 2H^+ \quad (2)$$

(M^{2+} is a divalent metal cation such as Hg^{2+} or Fe^{2+}). Under reducing conditions SRB, utilize SO_4^{2-}(Revis et al., 1991; Barnett et al., 1997) as a terminal electron acceptor (T.E.A.) in metabolic processes, subsequently releasing hydrogen sulfide (H_2S) as a by-product. The hydrogen sulfide is then free to react with divalent metal ions to form a metal monosulfide (Donald and Southam, 1999). Mercury present within the soil solution could potentially bind with sulfide forming either soluble or insoluble

complexes. According to Ravichandran et al. (1999), low pH values and sulfide concentrations promote the formation of insoluble HgS. It has been found that HgS will also form under alkaline conditions as well, however low redox potentials are required (Barnett et al., 1997). Conner (1990) reported that an excess of sulfide could increase the solubility of HgS and found that optimum HgS formation occurs at and below a 20% excess of the sulfide requirement.

Mercury has a high density and surface tension, therefore limiting mixing of sulfide and mercury for maximum interaction. However, mercury loading in HgS is quite high, a 24% to 28% molar ratio of sulfide to mercury produces HgS (Oji, 1998). Conversion of mercury and sulfide to HgS is an exothermic reaction (Table 1.2). Initially βHgS forms, a black amorphous powder, then as temperatures increase, conversion to αHgS, scarlet hexagonal crystals, develop:

$$Hg^{2+} + S^{2-} \rightarrow \beta HgS + \text{time or heat or pressure} \rightarrow \alpha HgS.$$

Table 0.2: Heats of Formation of HgS (Oji, 1998).

Form of HgS	ΔH_f° (kcal/mol)
αHgS	-13.90
βHgS	-12.90

HgS formation occurs in a sequence of steps: nucleation, growth of primary crystallites (few tens of nanometers in size), and aggregation of these microcrystals into larger (micron-sized) particles (Ravichandran et al., 1999).

Postgate (1984), reports that past experiments of HgS precipitation from mercury contaminated waste water have been met with some success however, it has been found that the addition of sulfate, in the form of calcium sulfate and generation of sulfide by SRB is far more effective versus direct additions of sulfide. When $CaSO_4$ is added to

soil, sulfate slowly dissolves and diffuses to depths reaching microbes and mercury. Sulfate stimulates metal sulfide formation and prevents the transformation of mercury into methylated or other organic forms (Revis et al., 1991). This method utilizes indigenous populations of microbes in anaerobic environments along with sulfate and labile carbon additions.

Addition of sulfate to anaerobic, mercury-contaminated soils may stimulate the production of methyl-mercury (Gilmour et al., 1992; Benoit et al., 1999; Benoit et al., 2001), depending upon sulfate and/or sulfide concentrations. Sulfate stimulates production of methyl mercury through enhancement of SRB activity (Benoit et al., 2001). However, higher sulfate concentrations (millimolar) have been shown to limit production of methyl mercury (Gilmour and Henry, 1991; Gilmour et al., 1992; Benoit et al., 2001). Gilmour and Henry (1991) suggest that there is an optimal sulfate concentration under which methylation of mercury occurs via SRB; methylation increases with sulfate concentrations up to 500 μM and decreases at higher concentrations. Production of sulfide (via sulfate reduction) inhibits methylation above this optimal concentration, whereas sulfate availability would limit sulfate reduction and subsequent mercury methylation below the optimum (Gilmour et al., 1992). Revis et al. (1989a) tested whether mercury chloride additions to soil could be converted to mercury sulfide via anaerobic incubation and found that up to 85% of the mercury chloride additions were converted to mercury sulfide, whereas only 0.01% was converted to methyl mercury.

The presence of DSOM enhances the solubility of cinnabar, resulting in a significant release of mercury into solution (Ravichandran et al., 1999). DSOM has an important function in the solubilization of mercury in all types of environments. It has

been suggested by Ravichandran et al. (1999) that concentrations and the nature of organic matter along with mercury concentrations dictate the extent of HgS formation and aggregation and inhibition in aquatic environments.

1.4.2 Benefits of Mercury Sulfide Formation

HgS is kinetically resistant to oxidation, therefore remaining solid under aerobic conditions and is one of the minerals with the slowest weathering rate in soil (Barnett et al., 1997). Of all metal sulfides, HgS (Table 1.3) is the least soluble.

Table 0.3: Ksp Values of HgS (Barnett et al., 1997).

Form of HgS	Ksp
αHgS	$10^{-36.8}$
βHgS	$10^{-36.3}$

Because HgS has such a low solubility, it potentially represents an important sink for mercury within the soil environment. Once HgS has formed within soils it remains stable indefinitely, and subsequently is of little or no risk to biological life forms via biological transformation and biomagnification (Revis et al., 1991). Revis et al. (1989a) observed growth of SRB in medium containing Hg^{2+}, with the majority of mercury being removed from solution (Table 1.4).

Table 0.4: Removal of Hg^{2+} from Solution by SRB (Revis et al., 1991).

Concentration of Hg		
Initial ppm	**Final ppm**	**Remaining %**
5.0	0.06	1.2
100	0.5	0.5

1.5 Purpose of Study

The primary objective of this study was to examine a novel biogeochemical technique to remediate mercury contaminated soils. I proposed to transform potentially

labile forms of mercury in contaminated soil to recalcitrant HgS by driving soils anaerobic in the presence of sulfate and SRB. Although the biogeochemical principles of this transformation are well established, the application of these principles and processes are yet to be demonstrated for mercury-contaminated soils, in which mercury occurs in a variety of forms (elemental, SOM bound, adsorbed, and inorganic mercury precipitates).

A secondary objective of this study was to determine which forms of soil mercury (water soluble, adsorbed, organic matter bound) are used in the formation of mercury sulfide. A four step sequential extraction (a modified version of Eganhouse et al. (1978)) was performed on the untreated soil and the treated and control soil after incubation. The forms of mercury identifiable by the extraction are:

1. Elemental mercury,
2. Water-soluble mercury,
3. Ion exchangeable mercury,
4. Organic matter associated mercury (including organic acids and bases), and
5. Soil mineral fraction associated mercury.

The results from the sequential extraction examined how anaerobic incubation of mercury contaminated soil changes the distribution of mercury within soil.

2.0 Materials and Methods

2.1 Soil Samples

Two bulk soil samples were obtained from the Turner Valley Gas Plant, Turner Valley, Alberta in October 2001. Samples were collected from the Absorber Building entrance (Kohut et al., 1995), based upon the source and degree of mercury contamination (Table 2.1). The source of contamination was elemental mercury released from manometers located within the Absorber Building. This contamination occurred repeatedly over several decades from the 1920's to 1987 when the plant was decommissioned. Samples were collected and then stored at room temperature in 40-L plastic buckets in the fume hood. The soils were air-dried, homogenized, sieved to 2 mm and then stored in 1-L plastic containers in the fume hood when not in use. Air drying and sieving of soil samples does not result in mercury losses (Kohut et al., 1995).

Table 2.1: Mercury Concentrations from Soil Samples Obtained from the Turner Valley Gas Plant (Kohut et al., 1995).

Sample Number	Hg (mg kg^{-1})	Soil Description
1	222	Loamy with some pebbles.
2	198	Loamy with a few rocks and many roots.

2.2 Routine Characterization

The particle size distribution was determined for the Turner Valley soil using the hydrometer method (Carter, 1993). The concentration of SO_4^{2-}, water-soluble carbonates and bicarbonates, total soluble iron (Fe) and manganese (Mn), electrical conductivity and redox potential were determined from a saturated paste extract (Dudas, 1988). The saturated paste was prepared by equilibrating approximately 250 g of air-dried, ground

soil with deionized water for 1 h. The solution was removed from the soil using vacuum filtration.

Sulfate concentration was determined using ion chromatography. The apparatus used was DX 600 ion chromatograph with an Ionpac AS9-H column (4 x 250 mm) and a CD 25 conductivity detector. Twenty-five μL samples were injected into a 9 mM sodium carbonate solution with a flow rate of 1 mL min^{-1}.

Soluble carbonates and bicarbonates were determined by titration (Dudas, 1988). Three to five drops of phenolphthalein was added to a 10mL sample of saturated paste extract water and titrated with 0.05 M HCl until the solution turned from pink to colorless. If the solution remains colorless upon the addition of phenolphthalein, this indicates an absence of carbonates. Three to five drops of Bromocresol green was then added to the water sample and titrated with 0.05 M HCl until the solution turned from blue to green to determine bicarbonate concentration. Total soluble iron and total soluble manganese concentrations were determined by ICP (inductively coupled plasma-atomic emission spectroscopy) at the Alberta Research Council in Vegreville. Electrical conductivity values of pore water samples were determined using a Model 31 Conductivity Bridge with electrical conductivity values adjusted to a 0.01 M KCl standard. Redox potential was measured using combination digital pH and mV meter equipped with a platinum oxidation-reduction potential (ORP) electrode. Redox potential (Eh) was determined from ORP values using the following formula:

$$Eh\ (mV) = ORP\ (mV) + 235\ (mV)$$

The pH of the soil was measured on a 1:2 soil: water mixture and a 1:2 soil: 0.01 M $CaCl_2$ (to determine reserve acidity) mixture using a digital pH meter with a glass electrode.

The total carbon content of the soil was determined using the Dumas Combustion Method and a NA 1500 Carlo-Erba elemental analyzer. The inorganic carbon fraction was removed through acid treatment with 6 M HCl, and the soil analyzed using the same method as total carbon, giving total organic carbon. The inorganic carbon fraction was calculated by subtracting the total organic carbon from total carbon.

2.3 Most Probable Number (MPN) Analysis

A MPN analysis was performed to determine if acetate-utilizing SRB were indigenous to the Turner Valley soil and if their numbers increased throughout the incubation. A modified Butlin's medium (Fedorak et al., 1987) was prepared, with of substitution of 2.0 g of CH_3COONa (sodium acetate) for sodium lactate. Several test tubes were prepared with 9 mL of medium and two iron nails. The tubes were capped with Kaput tops and were autoclaved for 20 min at 121 °C to sterilize them. Approximately 20g of soil was mixed in a sterilized blender with 180mL of sterile, distilled water for 2 min. The soil:water mixture was diluted from 10^0 to 10^{-10} using a sequential dilution procedure. The sterilized tubes were inoculated with 1 mL of diluted soil: water mixture from 10^{-1} to 10^{-10} with three tubes per dilution. The tubes were incubated in the dark for 1 month. After incubation the MPN tubes were scored. The presence of a black precipitate on the iron nails directly indicates the presence of SRB in the MPN tubes. The dilution factor and number of tubes within that dilution factor with a black precipitate (a positive score) were noted. Using a combination of positive scores,

the SRB population was then estimated using MPN tables from Standard Methods for the Examination of Water and Wastewater (1985). This same procedure was conducted on soil collected throughout the experiment.

2.4 Mercury Analysis

The mercury content of soil samples and solutions was determined using cold vapor atomic absorption (CVAA) by Alberta Research Council in Vegreville. The specific methods employed by ARC cannot be disclosed as they are propriety information and confidential. The following are summaries of the methods used by ARC.

2.4.1 Total Mercury in Sediments

A portion of soil or wet sediment was microwave digested with concentrated nitric and hydrochloric acids, converting inorganic and organic mercury to Hg^{2+}. Hydroxylamine hydrochloride solution was added and the sample was introduced into a flow injection system where Hg^{2+} was reduced to Hg^{o} by stannous chloride. The mercury vapour was swept with argon and passes into an atomic absorption cell for absorbance measurement. Sample absorbance was compared to the absorbance of a series of mercury standards and converted to mercury concentration in the sediment on a dry basis. The instrument detection limit (IDL) was 0.006 mg kg^{-1} and the method detection limit (MDL) was 0.016 mg kg^{-1}.

2.4.2 Total Mercury in Waters

Samples were digested with bromine chloride for 12 h at room temperature to convert all organic mercury to inorganic forms. After digestion, a hydroxylamine reagent was added to eliminate halogen interference. The sample solution was introduced into

the Flow Injection Mercury System and Hg^{o} vapor is produced by stannous chloride reduction. The mercury vapor was swept with argon into an atomic absorption cell. Sample absorbance was compared to the absorbance of a series of mercury standards and converted to mercury concentrations. The IDL and MDL for total mercury were 0.005 μg L^{-1} and 0.035 μg L^{-1}.

2.5 Microcosm Incubation

Two groups of microcosms were prepared, a control set and an experimental set. Both were incubated in 150 mL sterilized serum bottles using Teflon-lined butyl rubber stoppers to seal the bottles. Both sets of microcosms were amended with resazurin. Resazurin remains pink in the presence of oxygen and turns colorless in the absence of oxygen. It was used to detect air leaks in the microcosms. The microcosms were held anaerobic for specific time periods ranging from 1 to 36 wk, incubated in the dark and shaken daily. Following the incubation intervals, the microcosms were dismantled in triplicate. All transfers were made in a glove bag under a nitrogen atmosphere to prevent contamination with air. The microcosm contents were transferred to 250 mL centrifuge bottles and sealed with screw cap lids. After the transfers were complete, the centrifuge bottles were removed from the glove bag and centrifuged at 27 504 g for 20 min to separate the solids from the liquids. After centrifugation, the samples were returned to the glove bag and the redox potential was determined on the solids. The water decanted and filtered through a 0.22 μm nylon filter. The liquid samples were transferred to 60 mL glass sample bottles, amended with 0.182 g of manitol per 100 mL of liquid (to preserve sulfate – sulfide species present) and three drops of toluene (to prevent further microbial activity) and stored at 4°C (Alef and Nannipieri, 1995). Liquid samples were

analyzed for pH, electrical conductivity, sulfate concentration, total soluble iron and manganese and total carbonates and bicarbonates. The remaining soil was stored in 250 mL bottles and frozen until the following chemical analysis were performed: total mercury, nitric acid soluble mercury (HNO_3-Hg), sodium sulfide soluble mercury (Na_2S-Hg) (mercury sulfide), and residual mercury.

2.5.1 Control Microcosms

The control microcosms consisted of 50 g of mercury-contaminated soil and 125 mL of nitrogen-sparged, deionized water. Control microcosms were opened in triplicate on wk 0, 2, 11, 25 and 36.

2.5.2 Experimental Microcosms

The experimental microcosms consisted of 50g of mercury-contaminated soil, 125 mL of nitrogen-sparged, deionized water, 640 mg of calcium acetate ($Ca(CH_3COO)_2$) kg^{-1} soil, and 2.41 g L^{-1} of $CaSO_4$. Calcium acetate amendments were made to experimental microcosms on wk 8 and 25 to ensure an adequate carbon and energy source for microbial activity. Sets of three experimental microcosms were opened on wk 0, 1, 2, 3, 4, 5, 6, 11, 14, 21, 25, and 36.

2.6 Mercury Sulfide Extraction

Concentrations of HgS in soil were determined using a method described by Revis et al. (1989a; 1989b). The first series of steps removed all forms of mercury, except HgS. A 3 g sample of wet soil was placed into a 50 mL Teflon centrifuge tube along with 12 mL of 12 M of HNO_3 and agitated overnight at room temperature. The mixture was centrifuged at 47 807 g for 20 min and the supernatant removed. The soil

residue was washed with 12 mL of 12 M HNO_3 and centrifuged. The supernatants were combined, filtered and analyzed for total mercury, to give HNO_3-extractable mercury. The next series of steps extracted HgS from the residual soil. Twelve millilitres of saturated solution (SS)-Na_2S was added to the soil residue. The mixture was agitated overnight in a Teflon centrifuge tube. The mixture was centrifuged at 15 000 rpm for 20 min and the supernatant removed. The residue was washed with 12 mL of SS-Na_2S and centrifuged. The supernatants were combined, filtered and analyzed for total mercury, to give HgS.

2.7 Sequential Extraction

A four-step sequential extraction was used to determine the distribution of mercury in soil. A modified version of the method developed by Eganhouse et al. (1978) was used to determine concentrations of water-soluble mercury, ion exchangeable mercury, organic matter bound mercury (including organic acid and base bound mercury), and mercury in the mineral phase. One additional step was used in this study because the initial contamination of soil was from elemental mercury. Elemental mercury concentrations were measured by determining the total soil mercury content before and after thermal desorption (Renneberg, 2000). A 5 g soil sample was taken (in triplicate), with a 1 g sub-sample analyzed for total mercury. The remaining soil was placed in a 250 mL Erlenmeyer flask and placed on a hot plate, inside a fume hood, at 85°C for 16 h, causing any elemental mercury to volatilize (Renneberg, 2000; Windmoller et al, 1996). A 1 g sample of the thermally treated soil was analyzed for total mercury content. The elemental mercury content was determined by the difference between the thermally treated soil and un-treated soil.

The remaining three steps were performed in triplicate:

1. Water soluble Hg: 100 mL of distilled deionized water was added to 1.5 g of soil. The mixture was shaken for 30 minutes, centrifuged at 27 504 g for 20 min, and filtered (Glass Fiber filter paper). The filtrate was analyzed by CVAA.
2. Ion exchangeable Hg: To the residue 100 mL of 1 M $MgCl_2$ was added. The mixture was shaken for 30 min, centrifuged at 27 504 g for 20 min, decanted, and the extract analyzed by CVAA.
3. Organic matter associated Hg (OM): 50 mL of 30% H_2O_2 was added to 1.5 g of soil. Samples were digested at 85°C for 2 h. The contents were diluted to 100 mL using distilled deionized water, shaken for 30 minutes, centrifuged at 27 504 g for 20 min, filtered, and the filtrate analyzed by CVAA.
4. Mineral phase associated Hg: The residue from the above steps was analyzed by CVAA.

The sequential extraction was performed in triplicate on the untreated soil. This provided data on the initial distribution of anthropogenic mercury in the contaminated soil. After treatment of the contaminated soil through microcosm incubation, both the control (wk 36) and experimental (wk 20 and 36) soil underwent the sequential extraction. This provided data on the change in distribution of mercury in treated soils, specifically, allowing us to determine from which mercury fraction the mercury sulfide was formed.

2.8 Total Soluble Iron and Total Soluble Manganese Analysis

Total soluble iron and manganese was determined using ICP-MS at Alberta Research Council. The following is a summary of the method employed. Liquid samples

were 10-fold diluted using 0.23 M nitric acid and microwave digested at 165°C. After microwave digestion, samples were further 10-fold diluted using 0.23 M nitric acid. All measurements were carried out using a Perkin-Elmer ICP quadrupole mass spectrometer. The ICP-MS system was calibrated using standard solutions of 10 and 100ug L^{-1} of Fe and Mn in 0.23 M nitric acid. The IDL and MDL for iron were 3 $\mu g\ L^{-1}$ and 10 $\mu g\ L^{-1}$ and for manganese are 0.01 $\mu g\ L^{-1}$ and 0.08 $\mu g\ L^{-1}$.

2.9 Precipitate Analysis

A scanning electron microscope was used to examine surface morphology and elemental composition of precipitates formed during microcosm incubation. The precipitate was sprinkled onto double sided carbon tape to fix it to the sample holder. It was then coated in a Nanotek Srmprep sputter chamber with approximately 150 angstrums of gold. It was then placed in the sample chamber and observed with JSM-6301 field emission scanning electron microscope at 5 Kv for imaging and 20 Kv for x-ray analysis. Energy dispersive x-ray analysis (EDXA) was done with a PGT IMIX system.

2.10 Gas Analysis

Throughout incubation, microcosms were monitored for gas formation. A 20-gauge needle attached to a 10 mL syringe was inserted through the butyl rubber-Teflon lined stopper of the serum bottle. If a positive pressure existed within the microcosm, the headspace gas in the microcosm was tested for the presence of methane (CH_4) by gas chromatograph (GC) using the method outlined by Holowenko et al. (2000).

3.0 Results and Discussion

3.1 Soil Characteristics

The morphological and mineralogical information presented on the Turner Valley soil were gathered from Kohut et al. (1995). Soil survey maps of the Turner Valley area show the native soils at the Turner Valley Gas Plant to be disturbed throughout the industrial site (Scheelar, 1975). However, nearby soils have been mapped as Orthic Regosols, developed on a very gravely alluvial parent material. These soils have a shallow (5 to 9 cm) grey brown, calcareous humus enriched surface layer (Ahk) with a gravely loamy sand texture and pH of 7.0 to 7.5 (Kohut et al., 1995). The subsurface layer (Ck) has been characterized as gravely, grey and calcareous with a pH of 8.0 to 8.5.

The clay mineralogy of Turner Valley soils consists primarily of mica (illite) and kaolinite, with small amounts of chlorite and vermiculite (Kohut et al., 1995). The other minerals expected to be present include dolomite, sesquioxides, and quartz. The soil has a sandy loam texture with about 12% clay and a pH of 7.1. It contained 4.2% organic carbon, 6.0% total carbon and 1.8% inorganic carbon. The concentrations of major soluble components in saturated paste extracts of the Turner Valley soil are given in table 3.1.

Table 3.1: Pore water chemistry for the experimental soil.

Eh	E.C.	Ca*	Mg*	K*	Na*	SO_4^{2+}	HCO_3^-	Cl^{-*}	Total Fe	Total Mn
mV	$dS\ m^{-1}$	mg L^{-1}								
380	2.3	760	40	43	28	1200	300	23	2.4	0.1

E.C. = electrical conductivity, * Result obtained from Kohut et al., 1995.

The dominant clay is illite, which has a low cation exchange capacity (Kohut et al., 1995), therefore the amount of adsorbed mercury was not expected to be the dominant form of mercury. The organic matter fraction within the soil should primarily determine the amount of mercury adsorbed onto cation exchange sites. It is the organic matter quality coupled with quantity of organic matter that will determine the amount of mercury bound to exchange sites on soil organic matter. Organic matter quality is determined in part by vegetation growth on the soil. The native soils surrounding the Turner Valley Gas Plant are Black Chernozems, with a large build up of soil organic matter. The vegetation is primarily that of grassland species leading to soils with a high sulfur content organic matter. Based on the total organic carbon fraction, the organic matter content of the experimental soil is approximately 6.6%, typical for a Black Chernozemic soil.

The chemistry of the soil solution is dominated by sulfate and calcium. Geochemical modeling indicates that the soil solution is in equilibrium with calcium sulfate (gypsum) and therefore the calcium and sulfate concentrations are controlled by the solubility of gypsum (Kohut et al., 1995). Magnesium, potassium, sodium, chloride, total soluble iron and total soluble manganese are present at normal background concentrations for the soil type. The soil is aerobic, has a near neutral pH, and a moderately low electrical conductivity.

3.2 Initial Soil Mercury Distribution

The soil at the Turner Valley Gas Plant was contaminated with elemental mercury from the use of manometers. Contamination events occurred throughout the 60 years of operation of the gas plant, which ended in 1985. Elemental mercury spills were left in

place, and consequently the elemental mercury reverted to many soil-bound forms. The clay fraction (< 2 μm) contains the highest concentrations of mercury, whereas the sand fraction contains the lowest concentrations of mercury (Figure 3.1) (Kohut et al., 1995). Because the clay fraction has the greatest surface area and charge density versus the sand and silt fractions, the high concentration of mercury within this fraction indicates that adsorption of mercury to colloidal material is a dominant retention process for mercury in soil (Kohut et al., 1995).

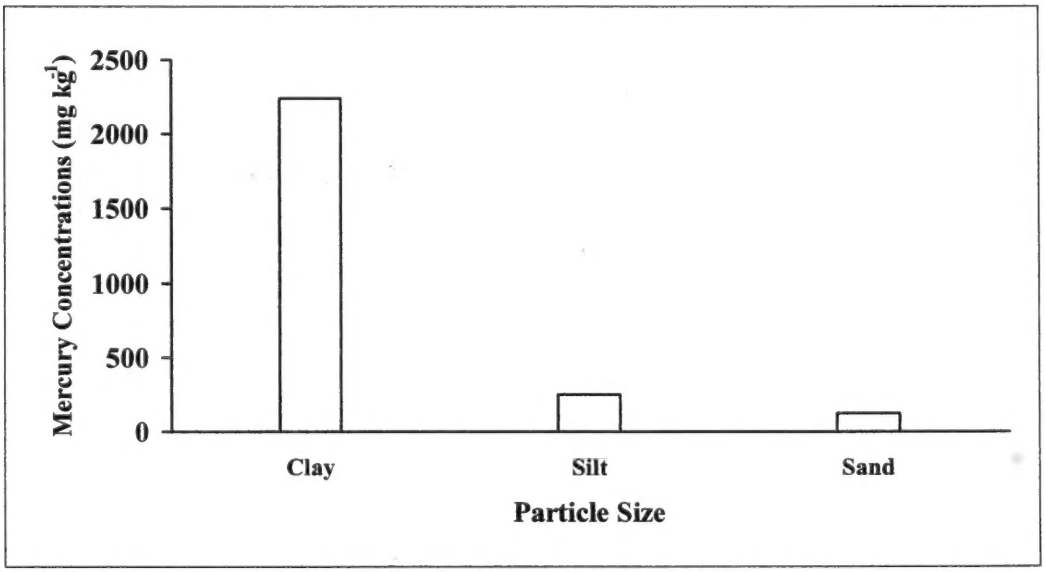

Figure 3.1: Distribution of mercury with particle size (Kohut et al., 1995)

The majority of total soil mercury prior to the microcosm incubation was found in the organic matter fraction (Figure 3.2). The mercury and soil organic matter reaction can be explained in part by the high cation exchange capacity of organic matter coupled with the many sulfur containing active sites of organic matter (Schuster, 1991; Renneberg and Dudas, 2001). It is also likely the mineral fraction contains some non-extractable forms of soil organic matter and it could be this recalcitrant organic matter that

contributes to the mercury concentrations recorded in the presumed mineral fraction. Due to its chemical nature, mercury has a strong affinity to sulfur and sulphur-containing functional groups. Organic matter contains several sulphur-containing compounds and functional groups, thus explaining the affinity of mercury to organic matter. Depending upon the organic matter properties and soil pH, mercury can also undergo chelation, inner and outer-sphere complex formation, adsorption and or co-precipitation (Schuster, 1991).

Mineral mercury contained the highest mercury content after organic matter. The mercury found in this fraction is likely to be found on the mineral surface bound to hydroxide, carbonate, phosphate, and sulfate containing minerals (Renneberg and Dudas, 2001). Water-phase and ion exchangeable mercury accounted for less than 1% of the total mercury. This is similar to the water-phase mercury concentration obtained by Kohut et al. (1995). However, Renneberg and Dudas (2000; 2001) found that up to 10% of total soil mercury could be found as water-soluble. Mercury sulfide also accounted for less than 1% of total mercury. It was expected that HgS would not be present initially because the Tuner Valley soil was an aerobic and well-drained surface soil. Elemental mercury was not detectable within the soil sample. It is likely that the elemental mercury has long since converted to other soil bound forms.

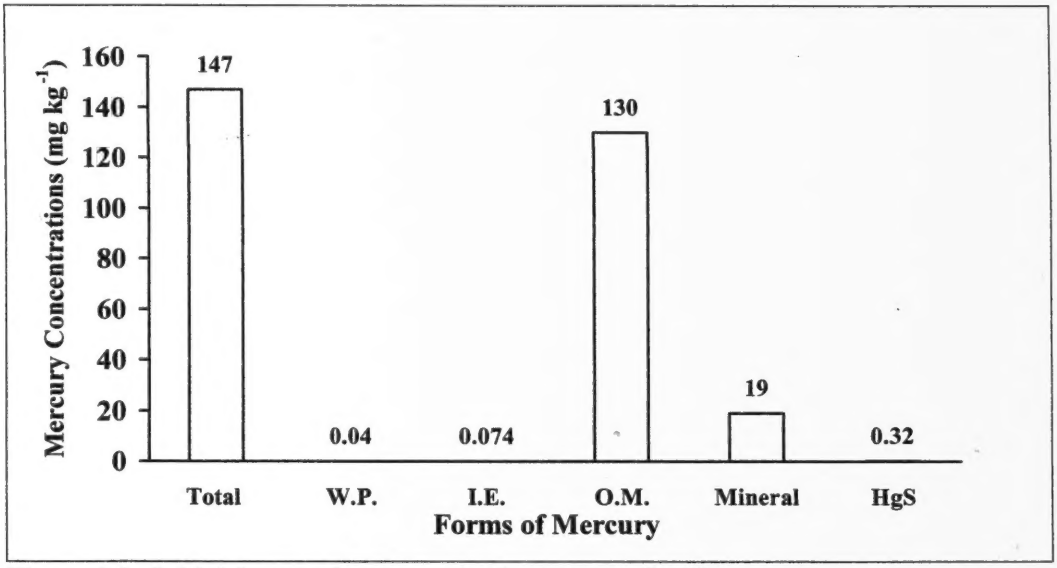

Figure 3.2: Initial forms of mercury in the untreated soil.

(W.P.-water-soluble Hg, I.E.-ion exchangeable Hg, O.M.-organic matter associated Hg, mineral –Hg associated with the soil mineral fraction).

Total mercury concentrations ranged from 120 to 170 mg kg^{-1} of soil (Table 3.2). Thirty-eight percent to 71% of total mercury was nitric acid removable in the mercury sulfide extraction outlined by Revis et al. (1989a). The background concentration of mercury sulfide was less than 1% (Table 3.3). According to Revis et al. (1989a) 98% of total mercury should be found in the nitric acid and sodium sulfide filtrates. However, only 38 to 69% of total mercury was found in these two filtrates. Therefore this extraction was not removing the soil mercury in its entirety. Based on research by Renneberg (2000) and Renneberg and Dudas (2001) up to 85% of total soil mercury can be found as organic matter bound. A portion of this organic matter bound mercury is likely bound to sulfur groups within the organic matter matrix, therefore it can be postulated that a portion of total soil mercury bound to sulfur groups within the organic matter has formed a pseudo mercury sulfide. It is then possible that this pseudo mercury

sulfide is not being extracted with the nitric acid or the sodium sulfide extractions. The soils used by Revis et al. (1989a) were from the East Fork Poplar Creek in Oak Ridge, Tennessee. Southern US soils tend to be highly weathered and low in soil organic matter, therefore very little of the total soil mercury would be present as organic matter bound mercury. It is likely then that the mercury present within those soils is in forms more available to participate in soil chemical reactions, including the formation of mercury sulfide.

Table 3.2: Results of the mercury sulfide extraction in the untreated soil.

Sample	Total Hg ($mg\ kg^{-1}$)	HNO_3-Hg ($mg\ kg^{-1}$)	HgS ($mg\ kg^{-1}$)
1	120	51	0.26
2	150	57	0.33
3	170	120	0.37
Average	**150**	**75**	**0.32**

3.3 MPN Analysis

SRB numbers (Table 3.3) were monitored throughout incubation in both the control and experimental soils. An increase in the counts of SRB is indicative of sulfate reduction (Abd-el-Malek and Rizk, 1963) leading to sulfide formation. In both the control and experimental microcosms SRB counts significantly increased throughout incubation, based on the statistical comparison outlined by Conchran (1950). There was no statistical difference between the SRB numbers in the control and experimental microcosms at wk 36.

Table 3.3: Numbers of acetate-utilizing SRB in the soil throughout incubation.

Time (wk)	Number of SRB g^{-1} soil
Wk 0 (untreated soil)	8.4×10^4
Wk 14 (experimental)	5.6×10^6
Wk 36 (experimental)	2.7×10^7
Wk 36 (control)	4.8×10^6

3.4 Microcosm Chemistry

3.4.1 Redox Potential

Control and $CaSO_4$ amended experimental microcosms (Figure 3.3) were prepared and allowed to incubate for 36 wk. At specific time intervals both the experimental and control microcosms were dismantled (in triplicate) and the soil and pore water extracted for detailed chemical analysis.

Figure 3.3: Photograph of a microcosm immediately after set-up.

The redox potential of the microcosms was measured under a nitrogen atmosphere using a platinum electrode (Figures 3.4 and 3.5). Initially, both sets of microcosms had a redox potential of 240 to 290 mV. The experimental microcosm redox potential dropped rapidly the first wk to -50 mV and the Eh fluctuated between 0 and -125 mV. At wk 5 a black precipitate (Figure 3.6) formed on the sides of the experimental microcosms, which when exposed to air for 24 h, turned rust (Figure 3.7). Analysis by scanning electron microscopy (SEM) showed the black precipitate to be amorphous and composed of iron and sulfur. Therefore, by wk 5, redox potentials within the experimental microcosms apparently reached levels conducive to sulfate reduction. During wk 6 to 21, the redox potential continued to drop, when at wk 21, with an Eh of -

230 mV the experimental microcosms began to crack due to increased pressure within the microcosms. Analysis of the headspace gas, by gas chromatography – mass spectrometry (GC-MS) showed the presence of CH_4. Therefore at wk 21 the experimental microcosms had reached redox potentials conducive to methanogenesis. Methanogenesis occurs when there is no longer any sulfate in solution to act as a terminal electron acceptor for microbial metabolic activities. Methanogens then begin using carbon dioxide as the terminal electron acceptor subsequently reducing it to methane. At wk 36, the end of incubation, the redox potential increased to -110 mV. Even though methanogenesis likely continued throughout the duration of the incubation, no increases in pressure were observed after wk 21.

The redox potential in the control microcosms also reached levels conducive to sulfate reduction at rates similar to the experimental microcosms. It was expected that he experimental microcosms would reach sulfate reduction more quickly due to the addition of calcium acetate, promoting increased microbial activity and subsequently faster reduction of microcosm redox potential. Control microcosms, on the other hand, did not receive any labile carbon amendments, therefore microorganisms had to rely on lower concentrations of carbon sources within the soil to carry out microbial activity. No black precipitate or gases formed during incubation of the control microcosms.

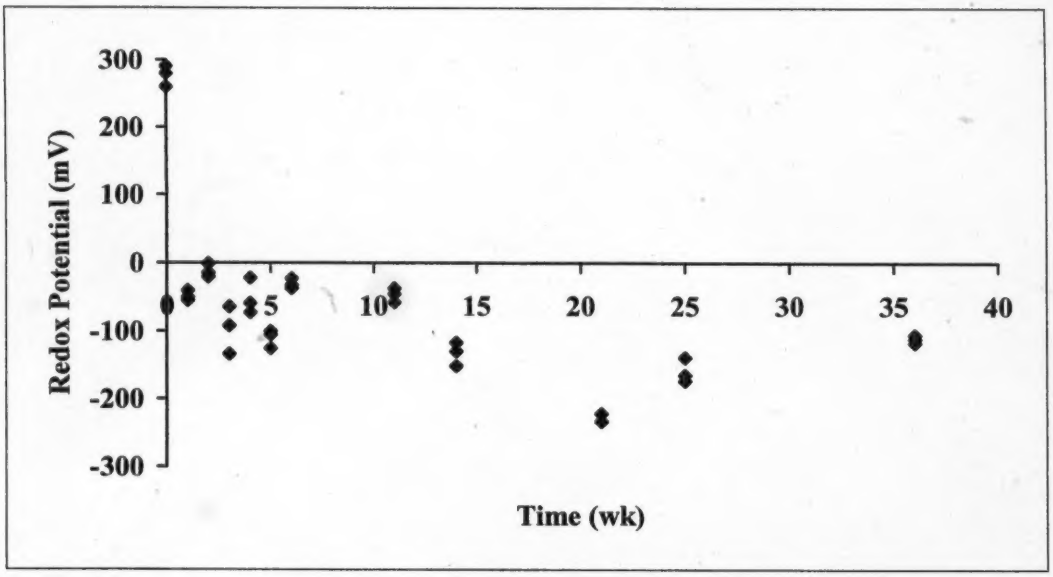

Figure 3.4: Redox potential of experimental microcosms throughout incubation.

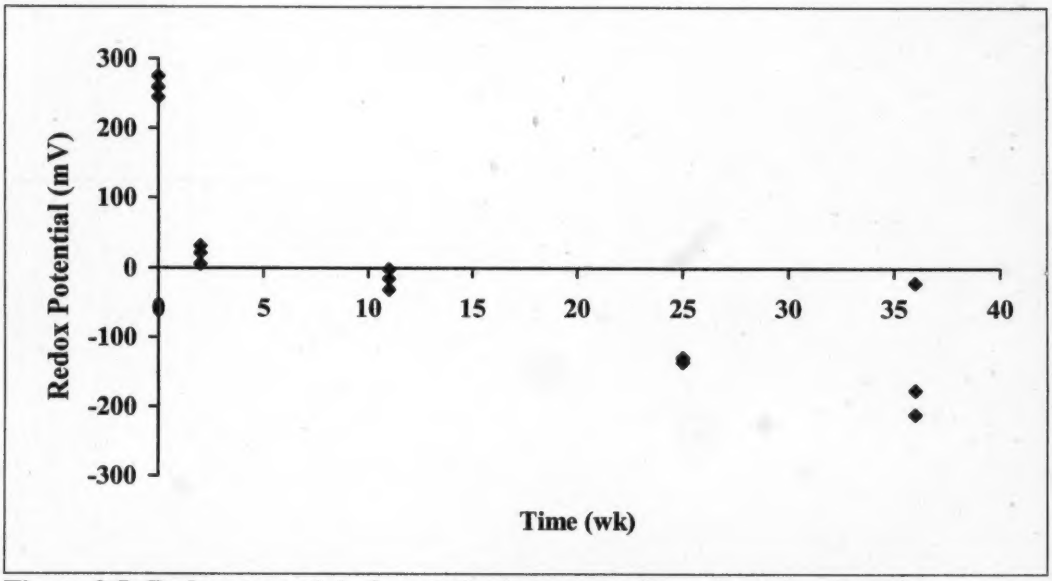

Figure 3.5: Redox potential of control microcosms throughout incubation.

Figure 3.6: Photograph of the black precipitate on the walls of an experimental microcosm.

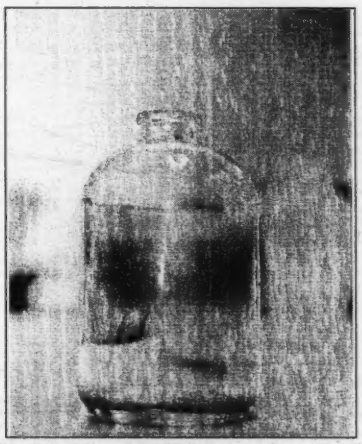

Figure 3.7: Photograph of the black precipitate after 24 hours of exposure to air resulting in a colour change from black to rust.

3.4.2 Electrical Conductivity

Electrical conductivity was monitored throughout incubation for both experimental and control microcosms. The background electrical conductivity of the Turner Valley soil is 0.4 dS m^{-1} (Kohut et al., 1995), which is very close to the initial electrical conductivity of the control microcosms (0.6 dS m^{-1}). Due to the additions of calcium acetate (640 mg kg^{-1} soil) and calcium sulfate (2.4 g L^{-1}), the initial electrical conductivity of the experimental microcosms was 2.2 dS m^{-1} (Figure 3.8). There was

concern that the additions of calcium acetate and calcium sulfate would result in salinization of the experimental microcosms thereby negatively impacting microbial activity. However, the electrical conductivity of experimental microcosms remained below 4 dS m^{-1} (considered the benchmark of salinity (Spositio, 1989) throughout the 36-wk incubation. In the experimental microcosms, there was a drop in electrical conductivity at wk 2 which can be explained by a drop in sulfate concentrations. During wk 3 E.C. increased to 2.3 dS m^{-1}, corresponding to increases in sulfate soluble iron and soluble manganese concentrations. The electrical conductivity for the experimental microcosms dropped during wk 4 and 5 to 0.7 and 0.5 dS m^{-1}. This corresponds to a drop in sulfate, soluble iron and soluble manganese concentrations. Also, at wk 5 amorphous iron sulfide formed as a black precipitate. Weeks 6 and 11 saw an increase in E.C. to 0.7 and 1.0 dS m^{-1}, as sulfate, soluble iron, and soluble manganese concentrations increased. During wk 14 to 36 the electrical conductivity was stable in the experimental microcosms.

Since there were no amendments made to the control microcosms, the initial electrical conductivity (Figure 3.9) was similar to that of background levels of the experimental soil. The E.C. remained stable during wk 0 and 2 (0.6 dS m^{-1}, 0.5 dS m^{-1}). At wk 11 E.C. increased to 1.1 dS m^{-1}, corresponding to an increase in soluble iron and soluble manganese concentrations. At wk 25 the E.C. dropped to 0.3 dS m^{-1}. This is similar to the E.C. drop seen in the experimental microcosms at wk 5. This could be explained by an increase in mercury sulfide concentrations, however, soluble iron concentrations more than doubled between wk 2 and 11, which should have lead to an

increase in electrical conductivity. Week 36 showed an increase in E.C. to 0.8 dS m^{-1}, corresponding to an increase in soluble iron and soluble manganese concentrations.

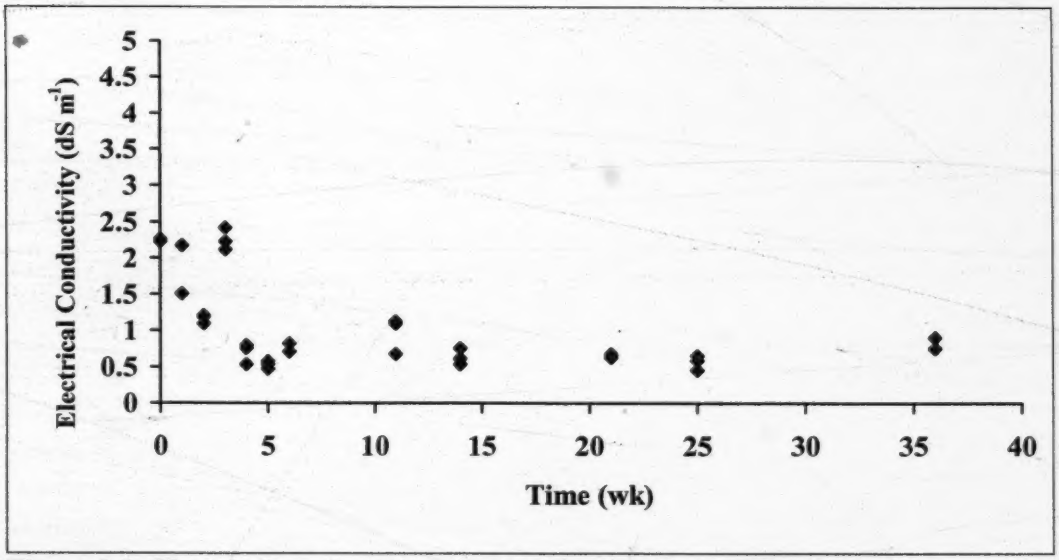

Figure 3.8: Electrical conductivity of experimental microcosms throughout incubation.

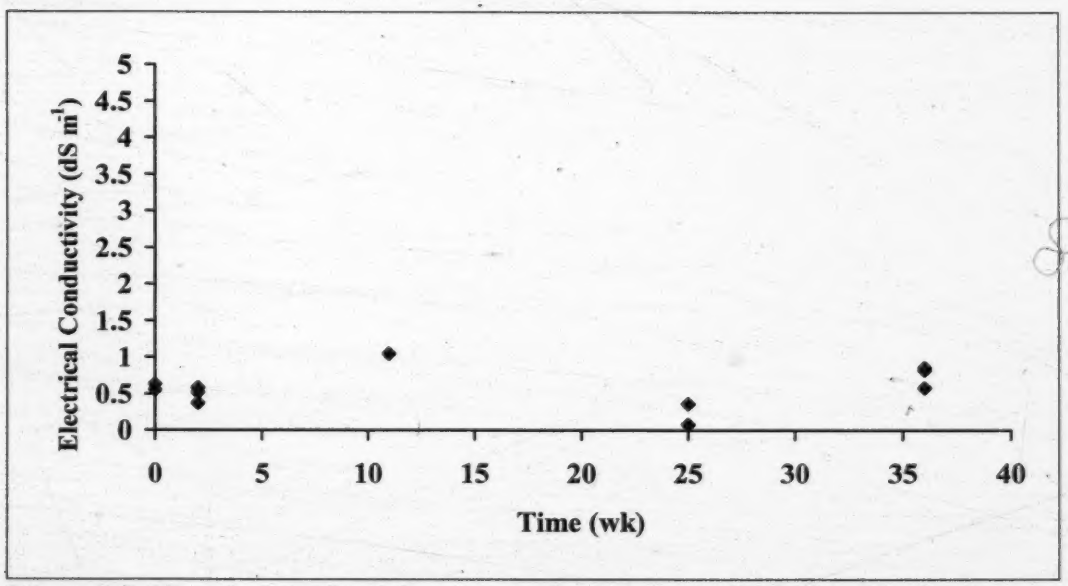

Figure 3.9: Electrical conductivity of control microcosms throughout incubation.

3.4.3 pH

The pH of the experimental microcosms (Figure 3.10) varied between 7.1 and 7.5 throughout the duration of the 36-wk experiment, which is similar to the background pH of 7.1. The pH of the control microcosms (Figure 3.11) varied between 7.3 and 7.4 throughout the incubation. This pH range is consistent with a calcareous soil with bicarbonate being the main form of inorganic carbon in solution (Salloum et al., 2002). Abd-el-Malek and Rizk (1963) found that sulfate reduction in soils is accompanied by a corresponding increase in pH, however the pH in both the control and experimental microcosms remained stable throughout the 36-wk incubation. These findings are similar to Salloum et al. (2002) where pH was observed to remain stable throughout the duration of the experiment.

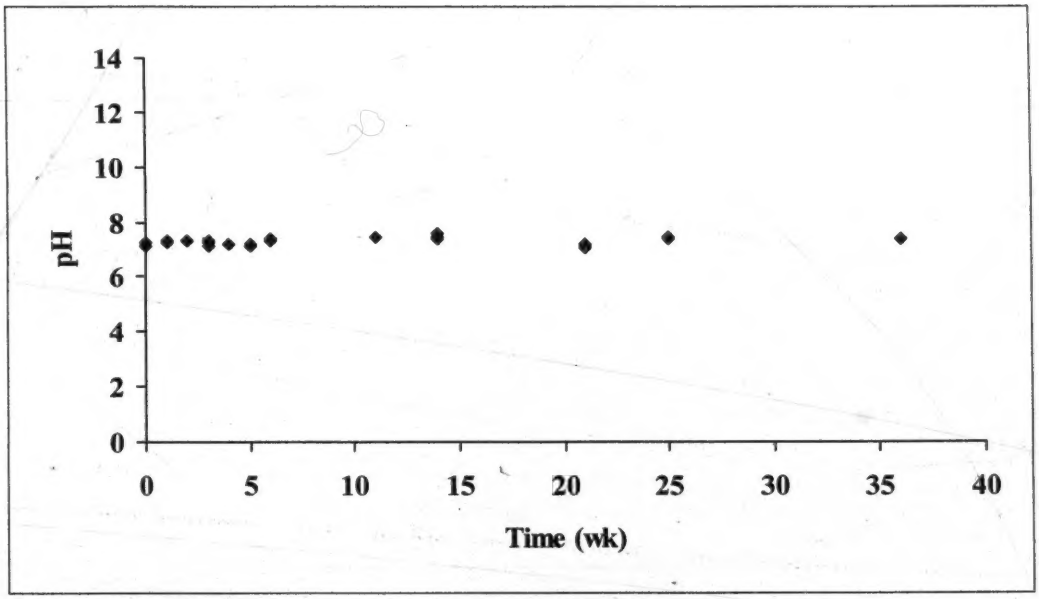

Figure 3.10: pH of experimental microcosms throughout incubation.

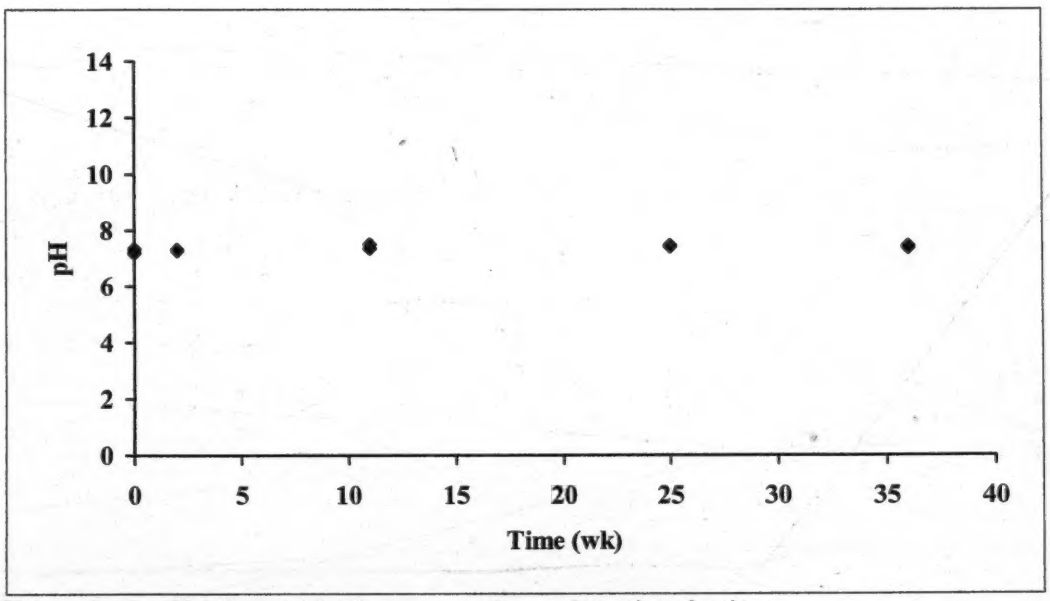

Figure 3.11: pH of control microcosms throughout incubation.

3.4.4 Sulfate Concentrations

Soluble sulfate concentrations were monitored for the experimental and control microcosms (Figure 3.12 and 3.13) throughout the 36-wk incubation. Background

concentrations for the soil samples were 1200 mg L^{-1}. At time = 0, after the addition of 2400 mg L^{-1} of calcium sulfate, the sulfate concentration for the experimental microcosms was 1200 mg L^{-1}. This was lower than expected. It was expected that all the calcium sulfate added would dissolve into solution, as the concentration added was based on the solubility of calcium sulfate in cold water. The complete dissolution of the calcium sulfate was likely inhibited by the addition of calcium acetate (the microbial carbon source) and the high background concentration of calcium (750 mg L^{-1}).

At wk 1, sulfate concentrations increased slightly to 1300 mg L^{-1}, dropped to 800 mg L^{-1} at wk 2, and returned to 1300 mg L^{-1} at wk 3. There was a significant decrease in sulfate concentrations to 400 mg L^{-1} at wk 4. Redox potentials reached levels conducive to sulfate reduction as early as wk 3; therefore the decrease in sulfate is likely due to sulfate reduction. Total soluble iron concentrations also dropped at wk 4 and a black precipitate identified as amorphous iron sulfide appeared at wk 5. Anaerobic incubation of soils amended with labile carbon and sulfate sources have undergone sulfate reduction and subsequent iron sulfide formation within 2 to 3 wk of incubation (Abd-el-Malek and Rizk, 1963). Therefore, iron sulfide formation during wk 4 of incubation and precipitation of iron sulfide during wk 5 is consistent with the literature. At wk 5 sulfate concentrations continued to decrease to 20 mg L^{-1}, however, soluble iron concentrations began to increase during wk 5, therefore this continued drop was not due to further iron sulfide formation. Nor was it due to hydrogen sulfide gas (H_2S) formation, as odor from H_2S was not detected in any of the microcosms. Sulfate-reducing bacteria have been shown to catalyze the conversion of amorphous iron sulfide (FeS) to pyrite (FeS_2) (Donald and Southam, 1999). It is thought that a thin film of amorphous iron sulfide

forms on the cell walls of SRB and that further reduction of sulfate and the subsequent release of H_2S promote FeS_2 formation (Donald and Southam, 1999). At wk 6 sulfate concentrations returned to 1200 mg L^{-1}. Because sulfate concentrations decreased below equilibrium at wk 4 and 5, the solid calcium sulfate was able to dissolve into solution until equilibrium was re-established. At wk 11 sulfate concentrations decreased slightly to 1100 mg L^{-1}, and remained constant through wk 14. At wk 21 sulfate concentrations decreased to 30 mg L^{-1}. The decrease in sulfate could not be due solely to mercury sulfide precipitations because the total mercury content is much less than what would be required for reaction with the sulfate. Since soluble iron concentrations increased and soluble manganese concentrations decreased only slightly during this period, they are not possible sinks for the sulfur. It is however possible that the sulfur was incorporated into organic matter through the formation of organo-sulfur compounds (Hartgers et al., 1997). High concentrations of reduced sulfur species relative to iron concentrations coupled with high counts of SRB and anoxic conditions can lead to the incorporation of sulfur species into soil organic matter (Hartgers et al., 1997). Conversion of amorphous iron sulfide to pyrite may have also occurred. Analysis of the iron sulfide at wk 21 by SEM (Figure 3.14) showed the concentrations of sulfur to iron to be approximately two to one. At wk 25 sulfate levels increased to 1100 mg L^{-1}, due to the continued dissolution of calcium sulfate. At wk 36 sulfate levels decreased slightly to 1100 mg L^{-1}.

Sulfate concentrations were also monitored within the control microcosms throughout incubation. Sulfate concentrations for time = 0 were 1200 mg L^{-1}, similar to that of background concentrations. At wk 2 sulfate concentrations increased slightly to 1400 mg L^{-1}, then decreased slightly at wk 11 and 25. At wk 36 sulfate decreased to

1200 mg L^{-1}. This slight drop in sulfate concentrations at wk 25 can be attributed to sulfate reduction due to the increase in mercury sulfide concentrations between wk 25 and 36. Though redox potentials do not confirm this; it is possible that sulfate reduction began taking place between wk 11 and 25 as an increase in mercury sulfide was observed during this time period. Since there was no carbon amendment to the control microcosms, microbial activity was slower within these microcosms, therefore taking the control microcosms longer to reach conditions conducive to sulfate reduction. I am assuming sulfate reduction began at wk 25 because that is when the redox potential reached levels conducive to sulfate reduction based on evidence from the experimental microcosms (FeS precipitate at wk 5).

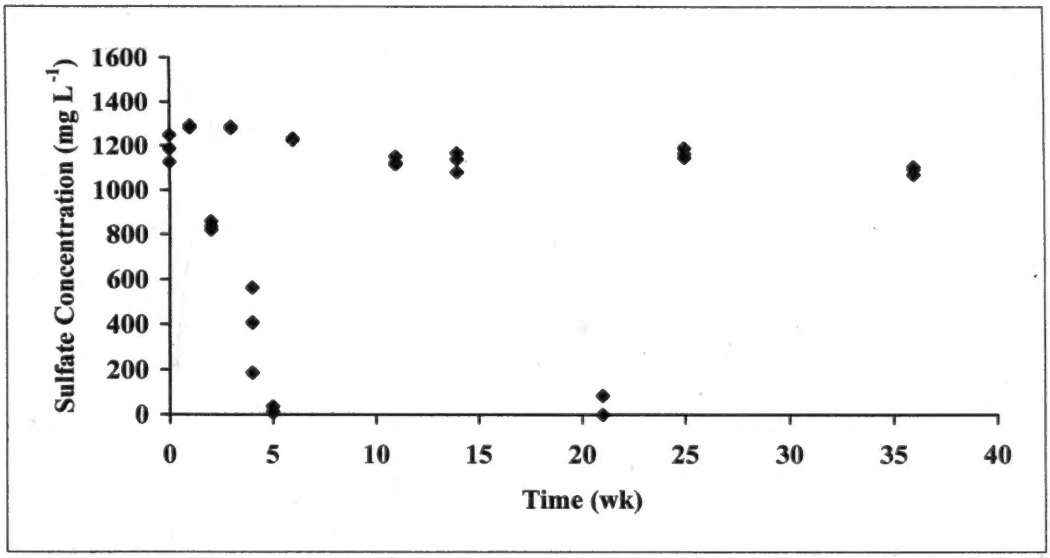

Figure 3.12: Sulfate concentrations of experimental microcosms throughout incubation.

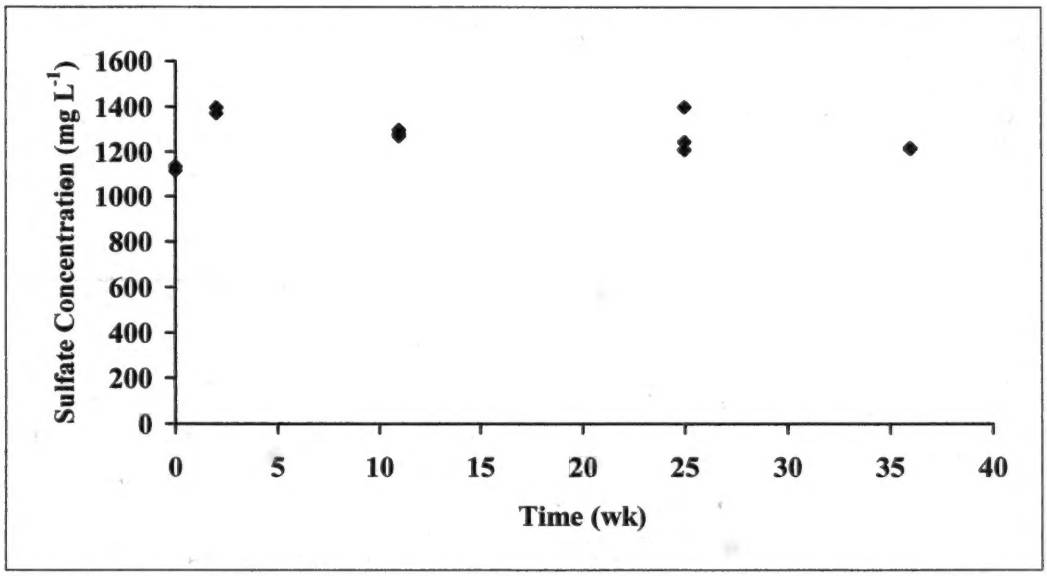

Figure 3.13: Sulfate concentrations of control microcosms throughout incubation.

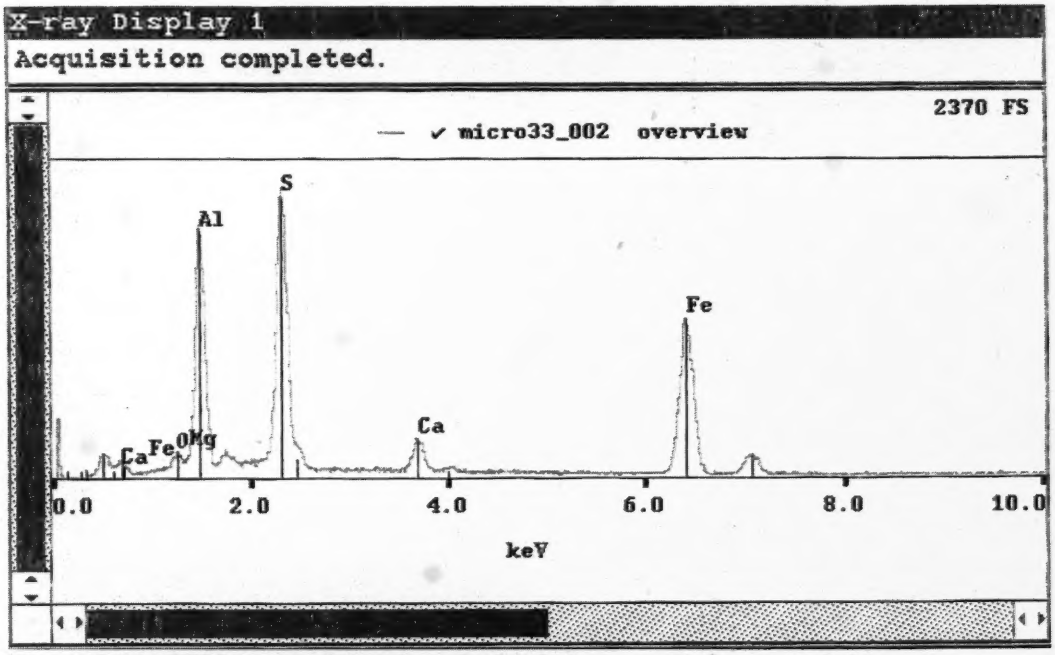

Figure 3.14: SEM compositional analysis of black precipitate at wk 21.

3.4.5 Bicarbonate Concentrations

Carbonate and bicarbonate concentrations were monitored for both the experimental and control microcosms throughout the 36-wk incubation. However, carbonate was not present in either the control or experimental microcosms. Bicarbonate was detected within both sets of microcosms, which is consistent with the pH range observed in the control and experimental microcosms. The formation of bicarbonate within the microcosms is a result microbial metabolic activity (Donald and Southam, 1999). Bicarbonate will form due to the oxidation of acetate by SRB:

$$CH_3COO^- + SO_4^{=} \rightarrow HS^- + 2HCO_3^-$$

Salloum et al. (2002) and Abd-el Malek and Rizk (1963) observed that as sulfate concentrations decreased, bicarbonate concentrations increased. This inverse sulfate-bicarbonate trend was observed in the experimental microcosms (Figure 3.15, 3.16) however the trend is not a gradual and continual decrease in sulfate and increase in

bicarbonates as observed by Salloum et al. (2002). Initially bicarbonate concentrations in the experimental microcosms are 300 mg L^{-1}, which was equal to the background concentration. During wk 1, bicarbonate concentrations increased slightly to 510 mg L^{-1}, however by wk 2, as sulfate concentrations began to decrease, there is a dramatic increase in bicarbonate concentrations to 3400 mg L^{-1}. At wk 3, sulfate concentrations increased, and bicarbonate concentrations decreased to 700 mg L^{-1}. This inverse sulphate-bicarbonate trend continued throughout the duration of the incubation. It would be expected that bicarbonate concentrations would gradually and continually increase during the 36-wk incubation with occasional jumps in concentration when sulfate levels dropped, versus the dramatic increases and decreases observed.

During wk 4, bicarbonate concentrations increase to 2100 mg L^{-1} as sulfate concentrations dropped. This trend continues in wk 5, where sulfate concentrations dropped to 19 mg L^{-1}, and bicarbonate concentrations peaked at 4300 mg L^{-1}. At wk 6, sulfate concentrations rose and subsequently bicarbonate levels decreased to 700 mg L^{-1}. By wk 11, sulfate concentrations decreased and bicarbonate concentrations increased to 1500 mg L^{-1}. At wk 21, sulfate concentrations dropped to 28 mg L^{-1}, and once again there was a dramatic increase in bicarbonate concentrations to 3200 mg L^{-1}. By wk 25 sulfate concentrations had recovered and bicarbonate concentrations dropped to 1900 mg L^{-1}. At wk 36, sulfate concentrations decreased slightly and bicarbonate concentrations increased to 2000 mg L^{-1}. It was observed that each time bicarbonate concentrations decreased, they never fell below the background concentration of bicarbonate, 300 mg L^{-1}. Therefore there was a net increase in bicarbonate concentrations throughout the 36-wk incubation.

The decreases observed in the bicarbonate concentration may also be due to the reaction and precipitation of bicarbonate with calcium (from the addition of $CaSO_4$ and $Ca(CH_3COO)_2$) to form calcium carbonate or calcite:

$$Ca^{2+} + HCO_3^- \leftrightarrow CaCO_3 \text{ (calcite)} + H^+$$

Bicarbonate concentrations increased when sulfate concentrations decreased (likely due to sulfate reduction). When soluble sulfate concentrations increased (due to the dissolution of $CaSO_4$), calcium concentrations in solution would have also increased. The calcium and bicarbonate could then react to form calcium carbonate, thus leading to a decrease in bicarbonate concentrations observed when sulfate concentrations increased.

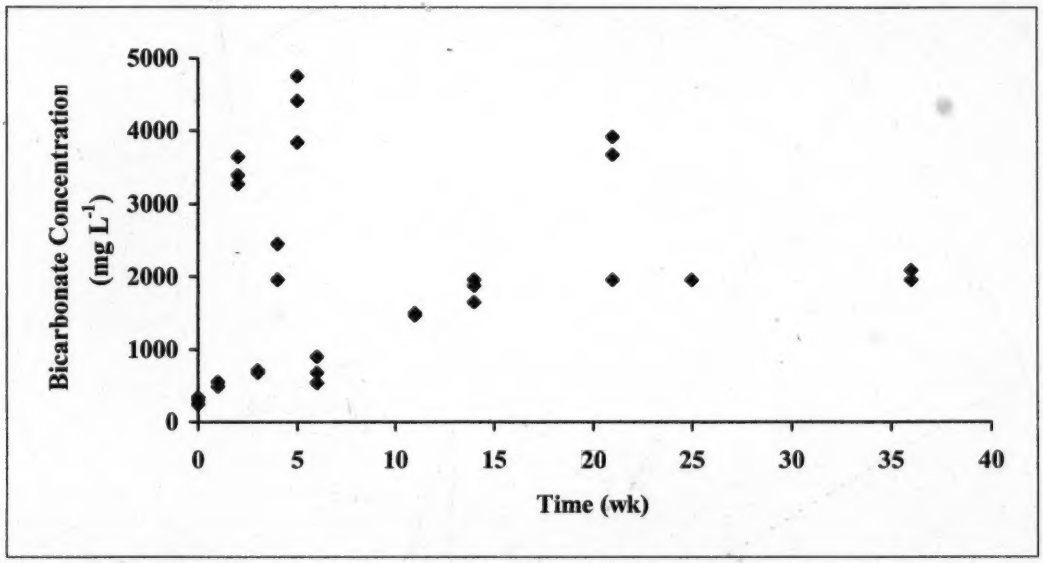

Figure 3.15: Bicarbonate concentrations of experimental microcosms throughout incubation.

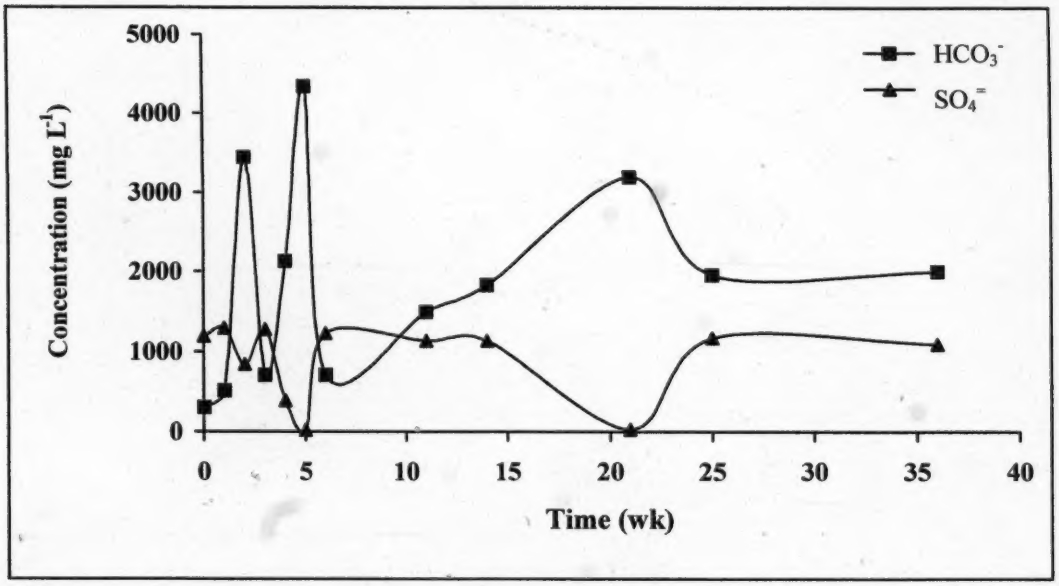

Figure 3.16: Mean bicarbonate and sulfate concentrations of experimental microcosms throughout incubation.

Unlike the experimental microcosms, bicarbonate concentrations for the control microcosms (Figure 3.17) followed a continuous and gradual upward trend throughout the first 25 wk of incubation. Initially bicarbonate concentrations (160 mg L^{-1}) were lower than the background bicarbonate concentrations (300 mg L^{-1}). By wk 2, bicarbonate concentrations had increased to 490 mg L^{-1}. Unlike the experimental microcosms, an inverse sulfate – bicarbonate trend was not observed in the control microcosms (Figure 3.18); there appears to be no obvious relationship between sulfate and bicarbonate concentrations in the control microcosms. Initially, as bicarbonate concentrations increase, sulfate concentrations increased as well. Between wk 2 and 11 there was a slight decrease in sulfate levels and an increase in bicarbonate concentrations to 970 mg L^{-1}. This is the only point in which the inverse sulfate-bicarbonate trend was observed in the control microcosms. There was no change in sulfate concentrations

between wk 11 and 25, however there was a doubling in bicarbonate concentrations to 1800 mg L^{-1}. Sulfate and bicarbonate concentrations dropped slightly during the final wk of incubation.

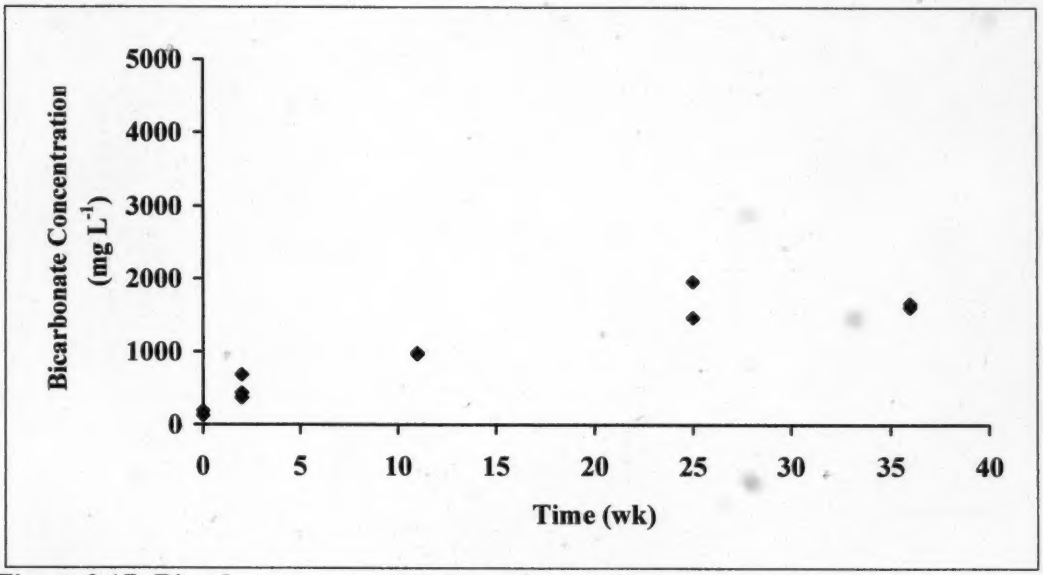

Figure 3.17: Bicarbonate concentrations of control microcosms throughout incubation.

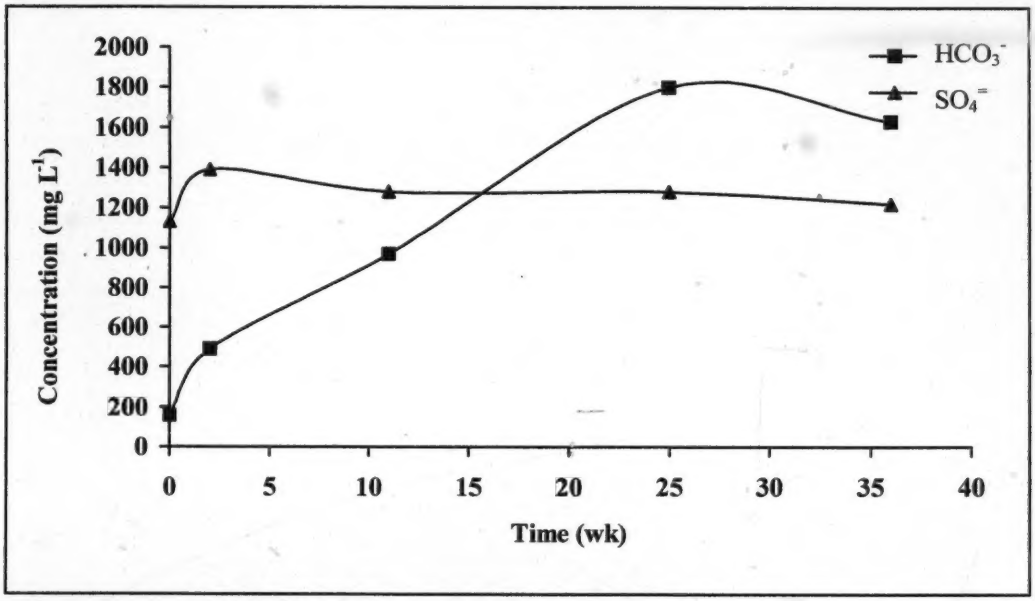

Figure 3.18: Mean bicarbonate and sulfate concentrations of control microcosms throughout incubation.

3.4.6 Total Soluble Iron

Total soluble iron and total soluble manganese concentrations were monitored in the control and experimental microcosms for two reasons. Fist, reduced iron (Fe^{2+}) and reduced manganese (Mn^{2+}) readily react with sulfide to form metal sulfides. Therefore, the reduced iron and reduced manganese may compete with mercury present within the soil solution for sulfide. Even though the formation of mercury sulfide is thermodynamically favored over the formation of amorphous iron sulfide (FeS) (Lindsay, 1979), pyrite (FeS_2), manganese sulfide (MnS) and hauerite (MnS_2), it may not be kinetically favoured. Observation of soluble iron and manganese concentrations also gives an indication of redox potential and the TEA being used by microorganisms. Second, the presence of ferrous iron in solution is a reliable indicator of anaerobic conditions within a soil. Iron reduction is considered the boundary between an aerobic and anaerobic soil (Bartlett, 1986).

Formation of iron carbonate (siderite) also provides a possible sink for soluble iron. Redox conditions were favorable to siderite formation at times throughout the 36-wk incubation. Iron carbonate is usually considered the dominant iron mineral to form under mildly reducing conditions, whereas iron sulfide and pyrite are the main minerals formed under low redox potentials (Krauskopf, 1967). However, iron carbonate formation is usually observed under conditions of high total carbonate (1 M) and low total sulfur (10^{-6} M) (Krauskopf, 1967). Increases and decreases in redox potential, as observed throughout the incubation of the experimental microcosms, may result in either the precipitation or dissolution of iron carbonate leading to fluctuations in soluble iron concentrations. In the experimental and control microcosms, high sulfur concentrations

and no carbonate was observed (only bicarbonate was detected), which favors the formation of pyrite versus that of siderite (Krauskopf, 1967).

Without comparison to sulfate concentrations, total soluble iron concentrations (Figure 3.19) do not appear to follow any trends throughout the incubation. Iron and sulfate (Figure 3.20) appear to have a relationship in the experimental microcosms, with wk 3, 4, 5 and 21 being of most significance. Initially, soluble iron concentrations were near zero. This was expected; at time 0 the microcosms were aerobic, and it is the reduced form of iron (Fe^{2+}) that is more soluble in water. As the microcosms become anaerobic, total soluble iron concentrations began to increase. By wk 1 soluble iron concentrations were 6.7 mg L^{-1} and by wk 2 and 3 soluble iron concentrations increased to approximately 13 mg L^{-1}. Between wk 3 and 4 there is a large decrease in total soluble iron (1.9 mg L^{-1}) and in sulfate. Redox potentials increased during this time period from –97 to –51 mV, though it is unlikely that the drop in iron is due to oxidation of Fe^{2+} to Fe^{3+}, as evidence of iron reduction began at wk 1 with an average redox potential of –48 mV. At wk 5 a black precipitate (Figure 3.21), identified as amorphous and presumed to be iron sulfide, was observed on the walls of the experimental microcosms. By wk 5, total soluble iron concentrations began to increase to 8.5 mg L^{-1}. They continued to increase, as did sulfate concentrations, to 12 mg L^{-1}at wk 6. Between wk 6 and 11, sulfide levels decreased along with total soluble iron concentrations to 6.7 mg L^{-1}. Most likely this decrease in both iron and sulfate were due to further iron sulfide formation. During wk 14 and 21, total soluble iron concentrations increased to 13.7 mg L^{-1} and 23.5 mg L^{-1}. During this period sulfate levels decreased to near zero. Because total soluble iron concentrations did not drop during this time, odor from H_2S was not detected, and

mercury sulfide concentrations were not high enough to account for the entire sulfate decrease, transformation of amorphous iron sulfide to pyrite may have occurred. For the duration of the incubation, total soluble iron concentrations decreased to 21.7 mg L^{-1} at wk 24 and 16.0 mg L^{-1} at wk 36.

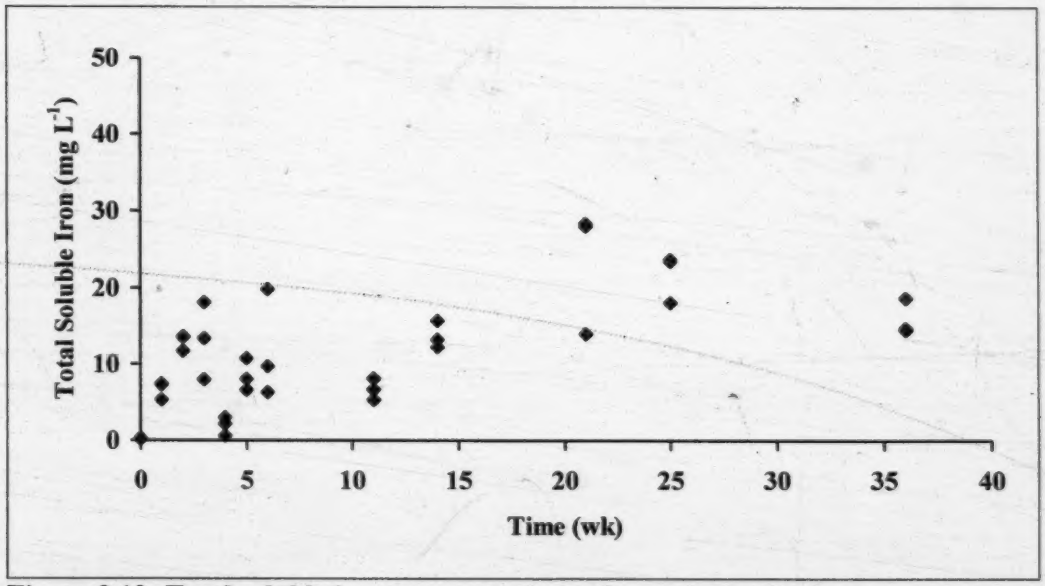

Figure 3.19: Total soluble iron concentrations of experimental microcosms throughout incubation.

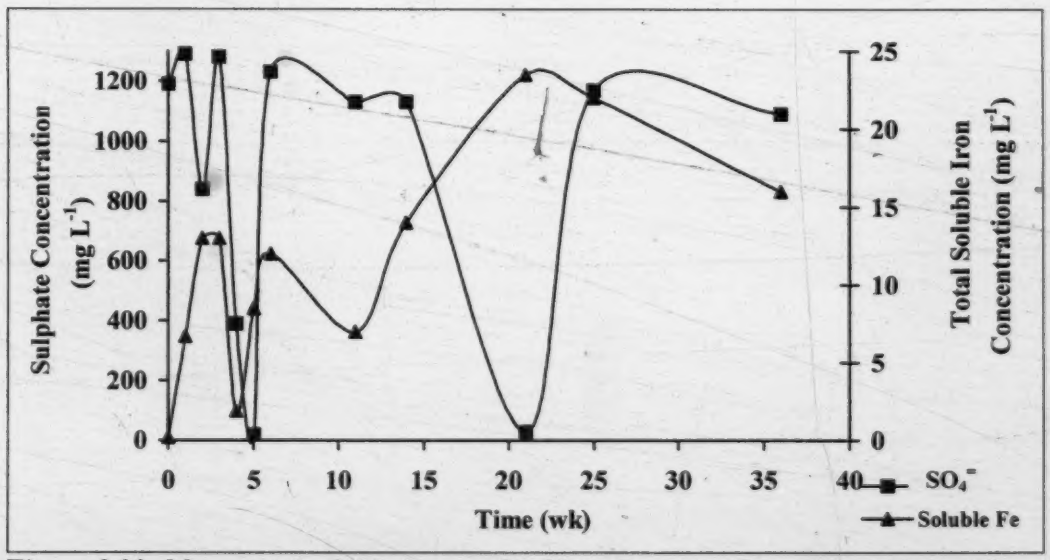

Figure 3.20: Mean total soluble iron and sulfate concentrations of experimental microcosms throughout incubation.

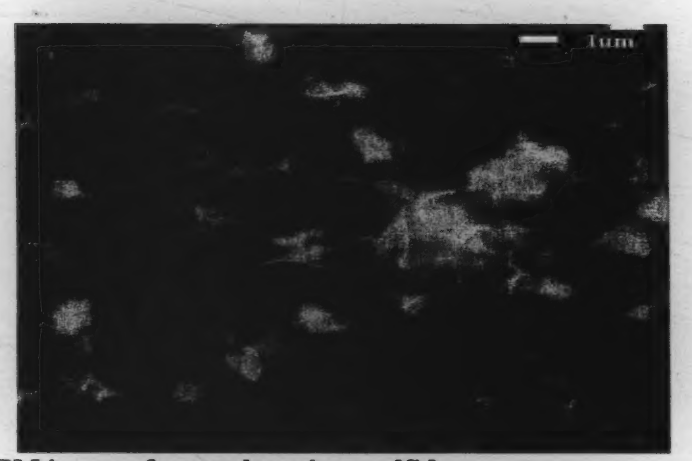

Figure 3.21: SEM image of amorphous iron sulfide.

Unlike the experimental microcosms, total soluble iron within the control microcosms (Figure 3.22) follows a continual and gradual upward trend throughout the 36-wk incubation. There was no black precipitate observed nor were there decreases in total soluble iron concentrations coupled with decreases in sulfate concentrations (Figure 3.23) as seen in the experimental microcosms. This is unusual because the redox potentials did reach levels conducive to sulfate reduction within the control microcosms and the increase in concentration of mercury sulfide coupled with increases in SRB numbers evidences the formation of sulfide within the control microcosms.

Acetate additions were made to the experimental microcosms to serve as an electron donor. Therefore because there was more electron donor in the experimental microcosms, more iron reduction occurred. With the presence of ferrous iron, coupled with the large decreases in sulfate (assumed to be due to sulfate reduction) iron sulfide formed in such quantities that precipitation occurred. It is likely that iron sulfide formed in the control microcosms, however concentrations were low until wk 20 and no decrease in sulfate was observed. Had incubation continued, it is expected that iron sulfide precipitate would have been observed in the control microcosms.

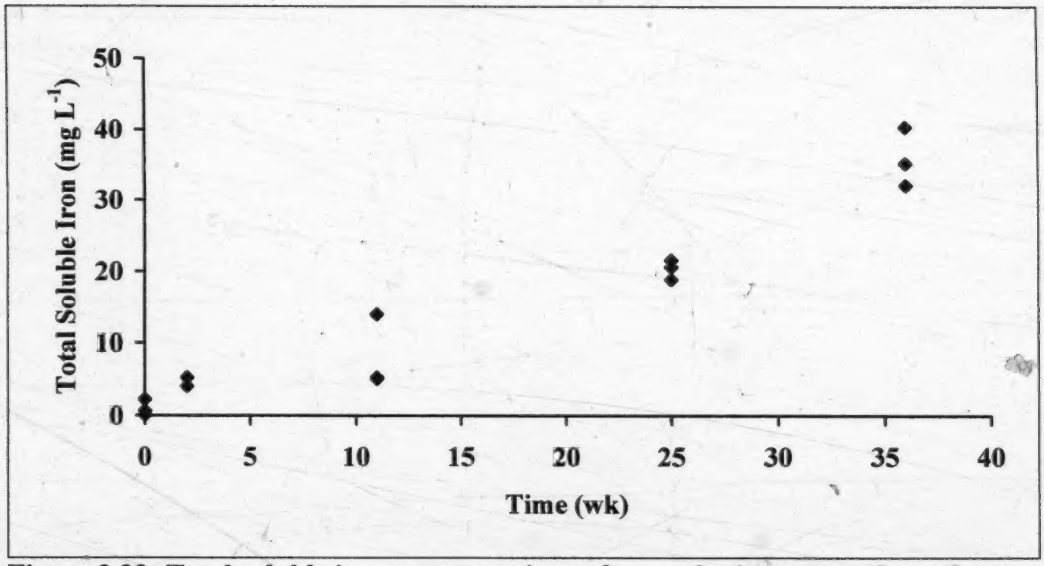

Figure 3.22: Total soluble iron concentrations of control microcosms throughout incubation.

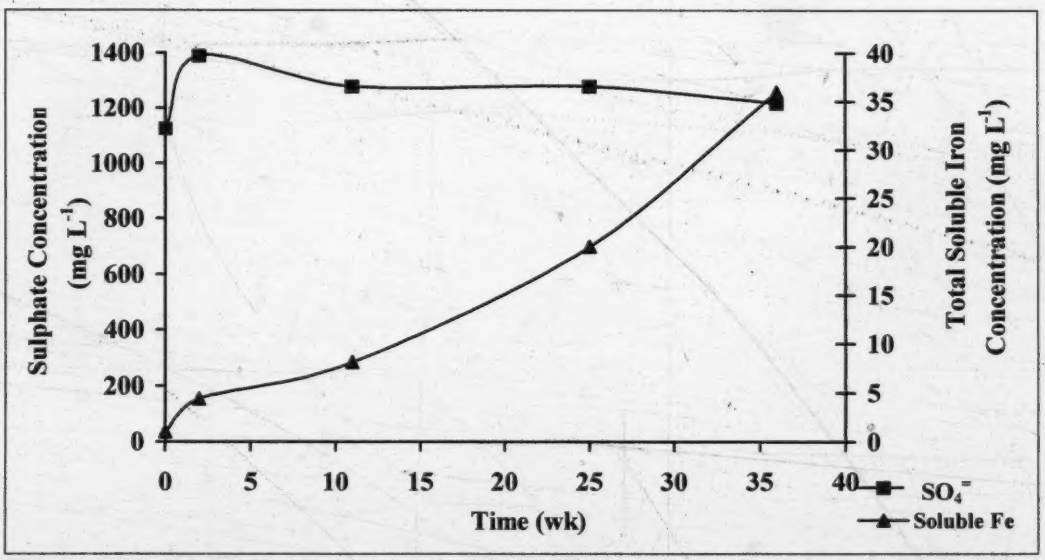

Figure 3.23: Total soluble iron and sulfate concentrations of control microcosms throughout incubation.

3.4.7 Total Soluble Manganese

Manganese, like iron, is a redox sensitive species and the presence of reduced manganese (Mn^{2+}) indicates moderately reduced conditions. Like iron, divalent manganese ion readily reacts with carbonate and sulfide to form minerals that are fairly

insoluble in basic to neutral pH conditions (Krauskopf, 1967). However, manganese sulfide is more soluble than iron sulfide and MnS_2 is much less stable than FeS_2 (Krauskopf, 1967). This may explain why no manganese was observed while analyzing the black precipitate formed in the experimental microcosms by EDXA. To promote manganese sulfide or disulfide formation, total sulfide concentrations must exceed carbonate concentrations by a minimum of a factor of 100 (Krauskopf, 1967). Carbonate was not observed and sulfate concentrations were high in the control and experimental microcosms. Manganese sulfide, disulfide or carbonate may have formed but not precipitated out of solution due to generally low soluble manganese concentrations. However, it is more likely that manganese sulfide or disulfide precipitates were simply not present in the sample of black precipitate analyzed by SEM-EDXA.

Unlike total soluble iron, total soluble manganese concentrations (Figures 3.24 and 3.25) within the experimental microcosms followed the sulfate trend closely. At wk 0, total soluble manganese concentrations were near zero. As the redox potential began to decrease, soluble manganese concentrations increased. Total soluble manganese concentrations peaked during wk 3 at 7.2 mg L^{-1}. At wk 4 total soluble manganese concentrations decreased to 0.7 mg L^{-1}. The same trend was observed in both sulfate and total soluble iron concentrations. It is likely that the soluble manganese precipitated as either manganese sulfide or bisulfide as did the soluble iron. Total soluble manganese concentrations then increased to 4.4 mg L^{-1} at wk 36.

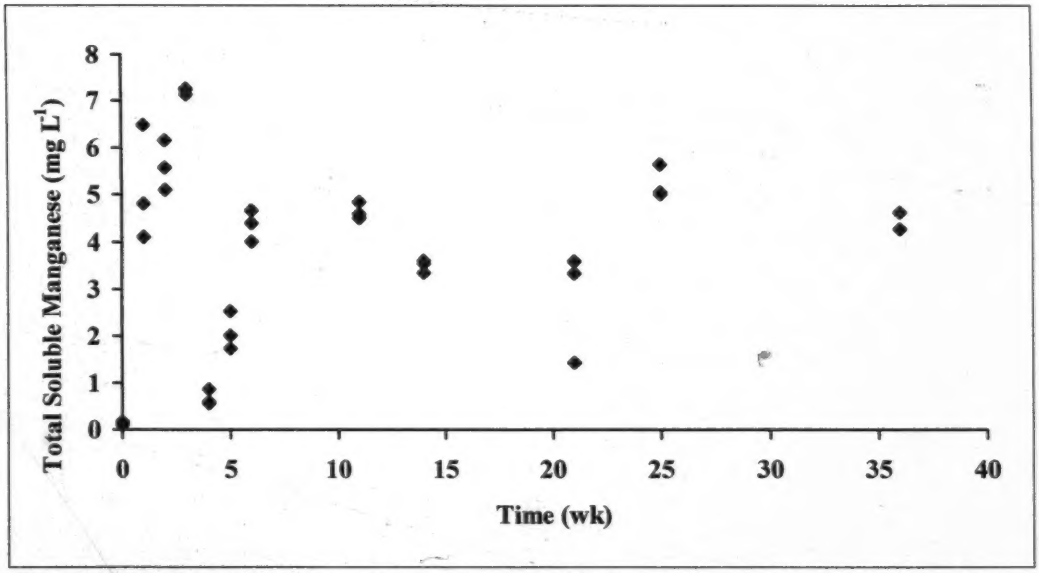

Figure 3.24: Total soluble manganese concentrations of experimental microcosms throughout incubation.

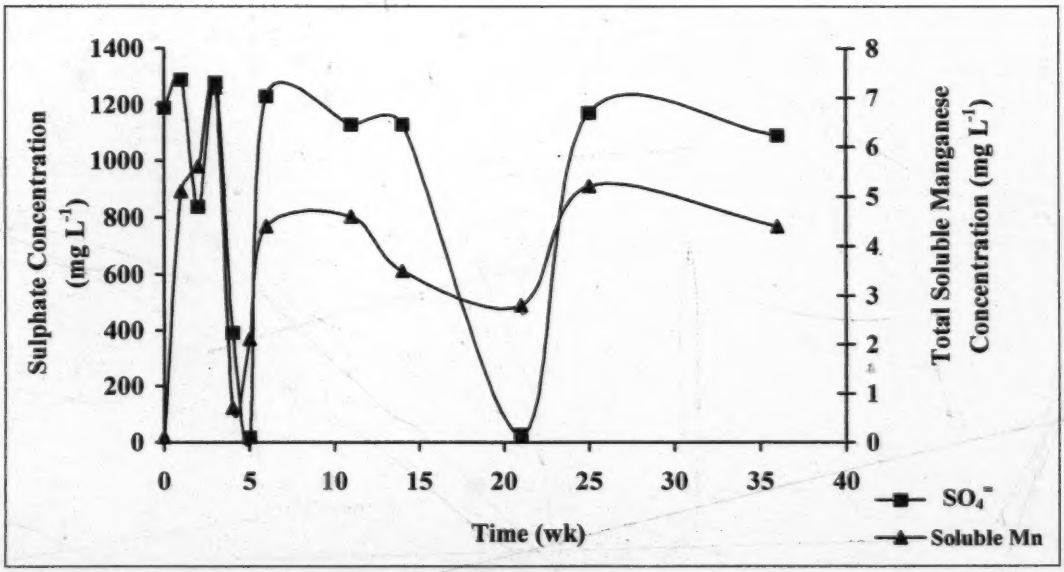

Figure 3.25: Mean total soluble manganese and sulfate concentrations of experimental microcosms throughout incubation.

Unlike the experimental microcosms, total soluble manganese concentrations (Figure 3.26, 3.27) paralleled sulfate concentrations in the control microcosms. At wk 0, total soluble manganese concentrations were near zero. As the redox potential began to decrease, total soluble manganese concentrations increased rapidly during the first 2 wk of incubation to 4.8 mg L^{-1}. As the incubation progressed, total soluble manganese concentrations continued to increase slightly to 6.8 mg L^{-1} at wk 36.

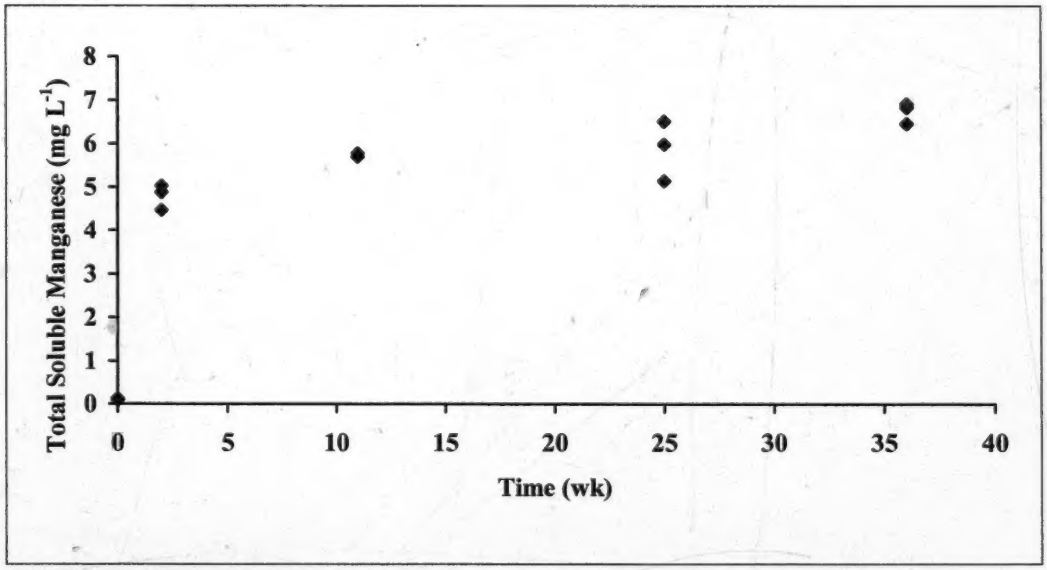

Figure 3.26: Total soluble manganese concentrations of control microcosms throughout incubation.

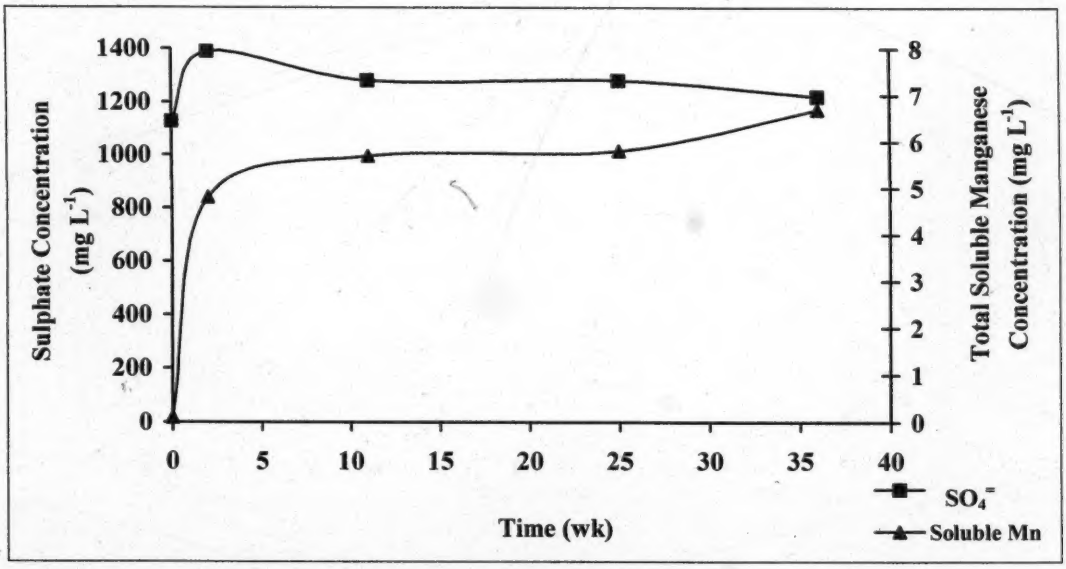

Figure 3.27: Mean total soluble manganese and sulfate concentrations of experimental microcosms throughout incubation.

3.4.8 *Methane Analysis*

During wk 21 the experimental microcosms were observed to have a high internal pressure evidenced by crack formation in the glass microcosms. Analysis of the headspace gas by GC revelled that CH_4 was present. Redox potentials did reach levels conducive to methane formation. In subsequent weeks, an increase in pressure within the microcosms was not observed. It is interesting to note that during methanogenesis, sulfate, iron, and manganese reduction was also simultaneously taking place. This contrasts with the notion that under specific redox conditions only a specific TEA can accept electrons and become reduced. However, soil and specifically these microcosms, are heterogeneous environments and it is not surprising that several terminal electron acceptors can accept electrons and become reduced simultaneously.

3.5 Microcosm Mercury

3.5.1 Total Mercury

Total mercury concentrations were determined at each sampling date in triplicate for the experimental (Figure 3.28) and control microcosms (Figure 3.29). There is considerable variability in total mercury concentrations within sub-samples and between sampling dates (microcosms). Mercury contamination at the Turner Valley Gas Plant occurred repeatedly over the several decades of operation with little or no attempt to clean up the elemental mercury spill. The spilled mercury remained within the top 20 cm of the soil with very little or no mercury detected below 20 cm (Kohut et al., 1995). Mercury contamination was therefore heterogeneous. Upon addition to the soil, the elemental mercury underwent various transformations, resulting in several different forms of mercury within the soil. This lead to "pockets" of contamination within the soil sampled from the Turner Valley Gas Plant. The soil samples were sieved to 2 mm and thoroughly mixed to reduce this heterogeneity, however, it is possible that soil mercury concentrations differed among microcosms due to the heterogeneous nature of the mercury contamination in the soil. Within the soil fraction there is further heterogeneity in mercury concentrations due to mercury distribution (organic matter bound, mineral bound, ion exchangeable etc.) and particle size distribution (sand, silt and clay). When microcosms were sampled and the contents centrifuged to separate soil solids and liquids, this heterogeneity became more pronounced. As samples were centrifuged, the heavier more dense particles (sands) settled out first with the finer, less dense particles (clays and organic matter) settling out last. According to Kohut et al. (1995), the clay-sized fraction contains the highest mercury concentrations versus the sand and silt-sized fractions. Furthermore, with up to 86% of soil mercury found as organic matter bound and 13% as

mineral bound (Figure 3.2), mercury concentrations would be highest in the top layer of particles in the centrifuge bottle. When soil samples were removed from centrifuge bottles, this variability in mercury concentration could not be eliminated. Therefore it is likely that some samples contained a greater proportion of clay and organic matter versus sand and silt. This could then lead to variability in mercury concentration between sub-samples from the same microcosm.

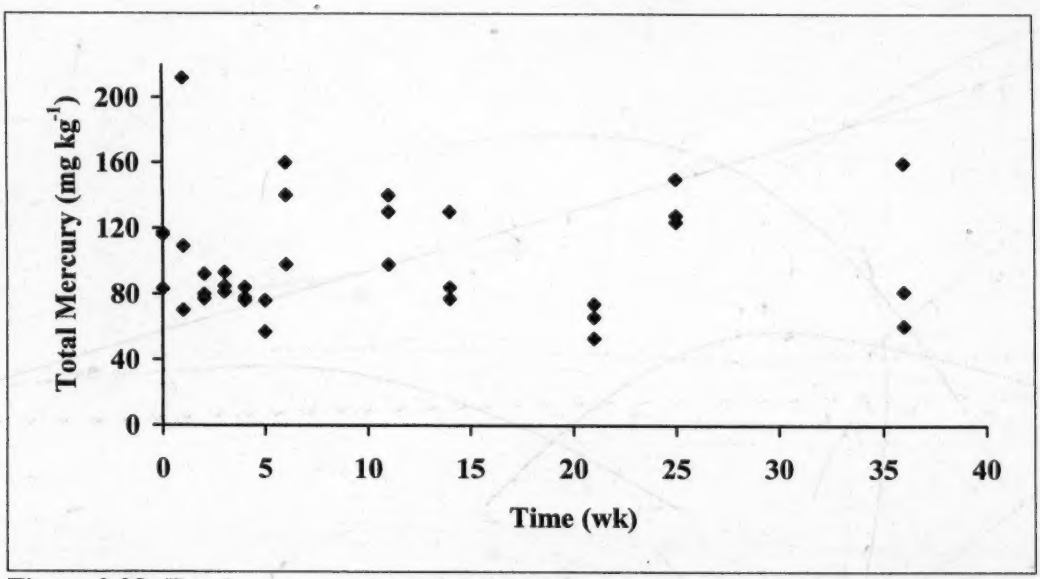

Figure 3.28: Total mercury concentrations in experimental microcosms throughout incubation.

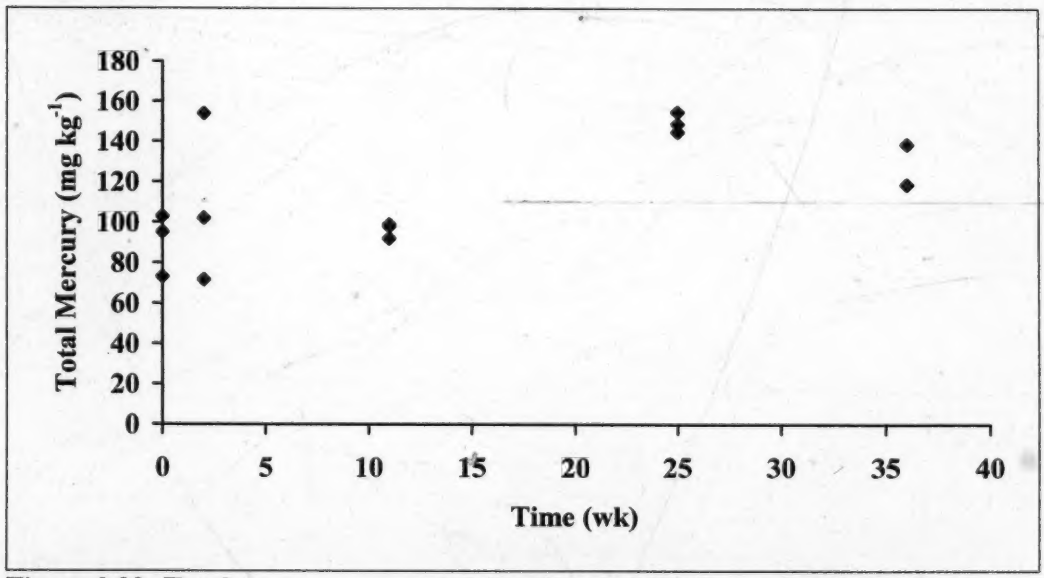

Figure 3.29: Total mercury concentrations in control microcosms throughout incubation.

3.5.2 Nitric Acid Extractable Mercury

Mercury sulfide concentrations were determined using a method outlined by Revis et al. (1989a). Mercury sulfide is insoluble in nitric acid and in aqueous solution (Revis et al, 1989a). To eliminate the other compounds and species of mercury from a

soil, it is agitated with nitric acid (termed nitric acid extractable mercury). The residue is then agitated with a saturated solution of sodium sulfide, which extracts the mercury sulfide. High concentrations of sulfide enhance the solubility of mercury sulfide (Morel et al., 1998; Wang et al., 1995). The remaining soil should then be essentially mercury free. Mercury concentrations can then be analyzed on the nitric acid and sodium sulfide filtrates. The concentration of mercury within these two filtrates should account for 98% of the total mercury present in the soil (Revis et al., 1989a).

Results of the nitric acid extractable mercury extraction in both the experimental microcosms (Figure 3.30) and the control microcosm (Figure 3.31) do not provide a definitive picture. Within the experimental microcosms, nitric acid extractable mercury concentrations varied considerably within microcosms and among microcosms. This variation is in part due to the variation in total mercury concentrations. It was expected that mercury sulfide concentrations would increase throughout incubation, therefore leading to an overall decrease in nitric acid extractable mercury concentrations. There is no significant decrease in the nitric acid extractable mercury within the experimental and control microcosms. However there is a 71% increase in mercury sulfide concentrations in both the control and experimental microcosms (Table 3.4).

Analysis of the residual soil, after extraction with nitric acid and sodium sulfide, showed up to 10 mg kg^{-1} of mercury. The extraction method did not remove all the mercury from soil samples. Only 38 to 69% of total mercury was accounted for in the nitric acid and sodium sulfide filtrates. As previously mentioned in section *3.2 Initial Soil Mercury Distribution*, mercury readily binds to sulfur groups within soil organic matter (87% of total soil mercury was found as organic matter bound), forming various

mercury – sulfur complexes and compounds. It is likely that these mercury –sulfur – organic matter complexes and compounds were not extracted with either the nitric acid or the sodium sulfide due to their chemical nature, and their physical protection by the humic structure of the organic matter (encapsulation of mercury –sulfur –organic matter complex within organic matter), therefore remaining in the residue. The quantity of organic matter within each microcosm and within each sub-sample likely varies. Consequently the amount of mercury – sulfur complexes and compounds varies within and between microcosms, leading to the variability in the nitric acid extractable mercury concentrations.

Methylation of mercury and subsequent volatilization upon microcosm dismantling could also account for differences between total mercury and the mercury present in the combined extracts. SRB are known biological contributors of methyl mercury formation (Gilmour et al., 1992; King et al., 2000), especially those capable of acetate utilization (King et al., 2002). However, under conditions of high sulfide concentration (millimolar), low levels of methyl mercury are frequently observed (Benoit et al., 2001). Benoit et al. (2001) hypothesize that high concentrations of sulfide inhibit mercury methylation by decreasing its bioavailability to SRB. Methylation of mercury decreased four-fold as sulfide concentrations increased from 10^{-6} to 10^{-3} M (Benoit et al., 2001). Concentrations of pore water sulfate ranged from 1.2×10^{-2} M to 1.9×10^{-4} M in the experimental microcosms and 1.4×10^{-2} M to 1.2×10^{-2} M in the control microcosms throughout the 36-wk incubation. Sulfide concentrations were not directly measured for pore water samples, however sulfide is known to have formed due to iron sulfide precipitate formation that was detected in the experimental microcosm. When sulfate

concentrations decreased, it can be assumed that sulfate reduction occurred. Therefore the sulfate concentrations observed can be directly correlated to sulfide concentrations. Furthermore, Revis et al. (1989a) found when sulfate additions were made to mercury chloride contaminated soil and incubated under anaerobic conditions, 0.01% of the mercury chloride was converted to methyl mercury.

Morel et al. (1998) stated that methylation reactions can be the result of photochemical processes involving acetate or humic acids. However, this is unlikely as all microcosms were incubated in the dark.

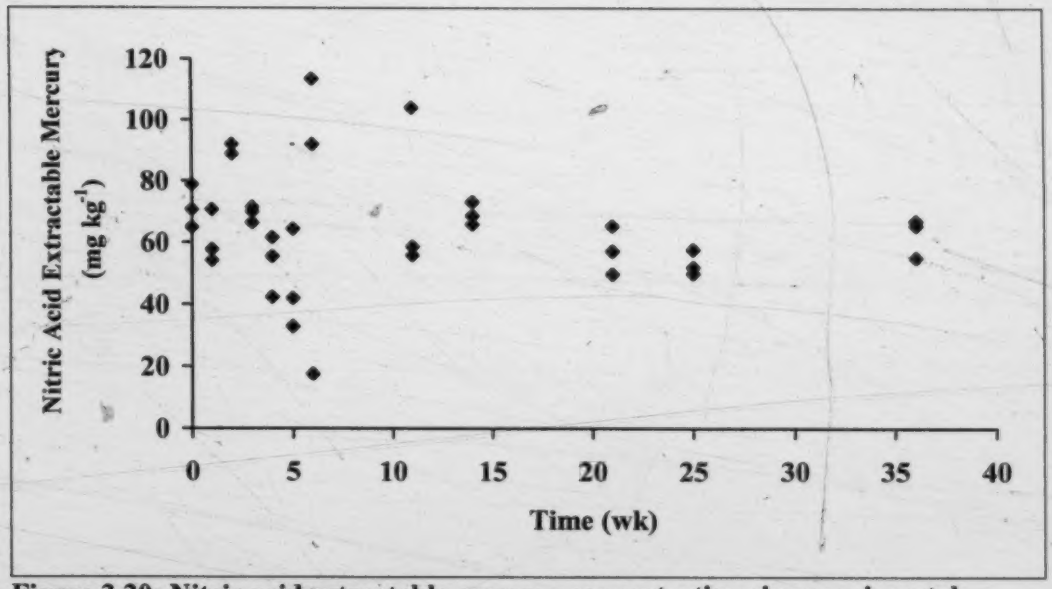

Figure 3.30: Nitric acid extractable mercury concentrations in experimental microcosms throughout incubation.

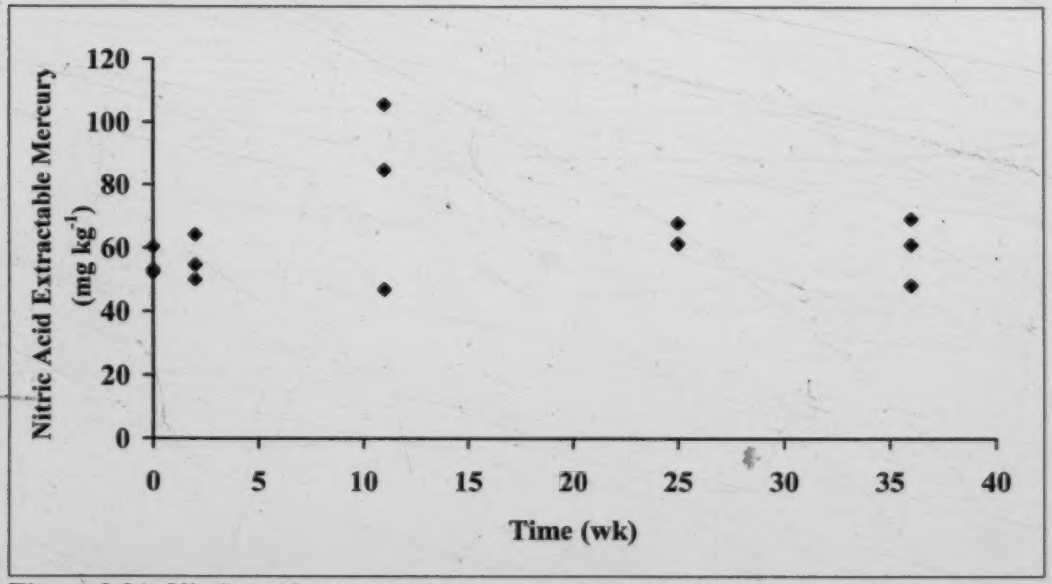

Figure 3.31: Nitric acid extractable mercury concentrations in control microcosms throughout incubation.

3.5.3 Mercury Sulfide

Throughout the 36-wk incubation, mercury sulfide concentrations increased in both the experimental (Figure 3.32) and control microcosms (Figure 3.33) by 71% (Table

3.4). However, only 11% of total mercury was found as mercury sulfide in the experimental microcosms and only 8.1% in the control microcosms at wk 36. This is much lower than expected. Revis et al. (1989a) found that up to 85% of mercury chloride was converted to mercury sulfide, and that between 73 and 90% of total mercury was found as mercury sulfide in a floodplain soil. Conversion of mercury chloride to mercury sulfide should yield high conversion rates, because the mercury is present in solution and in a form readily available for chemical reaction (i.e. Hg^{2+}).

Like the Turner Valley soil, the floodplain of East Fork Poplar Creek was contaminated with elemental mercury with large-scale mercury releases ending in the 1960s (Barnett et al., 1997). Overtime, the mercury within the floodplain soil has likely reverted to a variety of forms (organic matter bound, mineral bound, water soluble, ion exchangeable), therefore similar to the mercury within the Turner Valley soil. It was expected that the Turner Valley soil would yield similar ratios of mercury sulfide to total mercury as the floodplain soil examined by Revis et al. (1989a) after the 36-wk anaerobic incubation. Though not known for sure, it can be postulated that the soil examined by Revis et al. (1989a) contained much less soil organic matter than the Turner Valley soil. Native soils of the southern U.S. are typically strongly weathered soils with minimal accumulation of soil organic matter. Therefore it is likely that the mercury found in the East Fork Poplar Creek soil was present in forms (water soluble and ion exchangeable) more available for chemical reaction (i.e. not organic matter bound). The soil mercury found at the East Fork Poplar Creek site has undergone periodic reducing conditions for more than 4 decades, whereas the Turner Valley soil was held anaerobic for 36-wk. Furthermore the East Fork Poplar Creek soil was anaerobic upon initial mercury

contamination and it is possible that the mercury was converted to mercury sulfide before it reverted to the other soil bound forms observed in the Turner Valley soil.

When sulfide is present in sufficiently high concentrations it can lead to increased solubility of mercury sulfide due to the formation of dissolved sulfide and bisulfide – mercury complexes (Morel et al., 1998; Wang et al., 1995). Background sulfate concentrations for the Turner Valley soil were 1200 mg L^{-1}, with additions of 2.41 g L^{-1} of calcium sulfate made to the experimental microcosms. Background concentrations of sulfate for the East Fork Poplar Creek floodplain soil were 22 mg kg-1 of wet soil. It is possible that both the control and experimental microcosms had an excess of sulfide, which resulted in the formation of soluble mercury – sulfur complexes versus the formation and precipitation of mercury sulfide. According to Figure 3.28 and Tables 3.4 to 3.6 the distribution of soil mercury did not change significantly throughout the 36-wk incubation. Therefore, if soluble complexes of mercury and sulfur were forming, they would be low in quantity due to a lack of change in mercury distribution (i.e. there were major changes in mercury distribution – therefore no readily available source of mercury for these complexes).

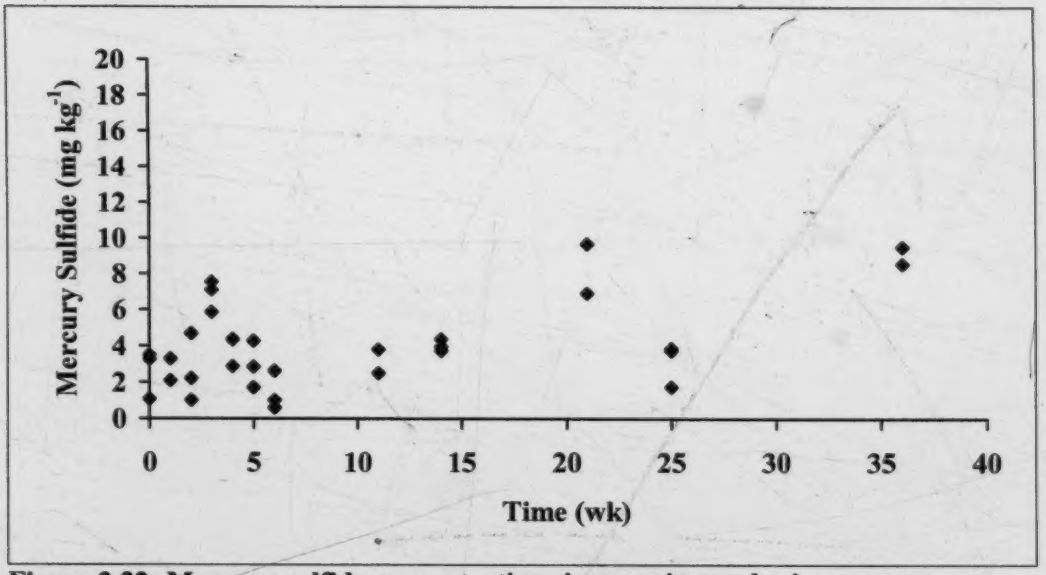

Figure 3.32: Mercury sulfide concentrations in experimental microcosms throughout incubation.

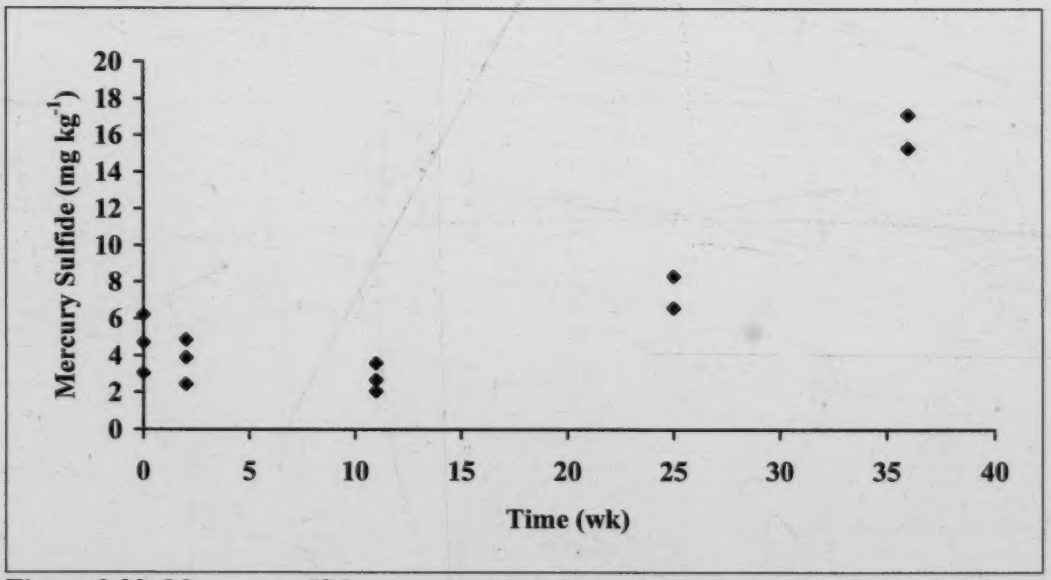

Figure 3.33: Mercury sulfide concentrations in control microcosms throughout incubation.

Table 3.4: Change in mercury sulfide concentration throughout the 36 wk incubation.

Soil	HgS (mg kg-1)		% Change	Significantly different (Y/N)*
	Wk 0	Wk 36		
Control	4.7 ± 1.8	16.2 ± 1.8	+71	Y
Experimental	2.6 ± 1.5	9.0 ± 0.91	+71	Y

* T-test where $\alpha = 0.05$.

There was no significant change in mercury distribution (Figure 3.34, Tables 3.5, 3.6) throughout the 36-wk incubation. The apparent changes in organic matter bound mercury correspond with the differences observed in the total mercury concentrations. With such a large proportion of total mercury found as organic matter bound mercury both pre and post incubation it is likely that soil mercury held as organic matter bound mercury is stable and unlikely chemically available. Sites where the majority of mercury is organic matter bound may not need any further method of mercury stabilization until a suitable remediation method is employed or the site is excavated.

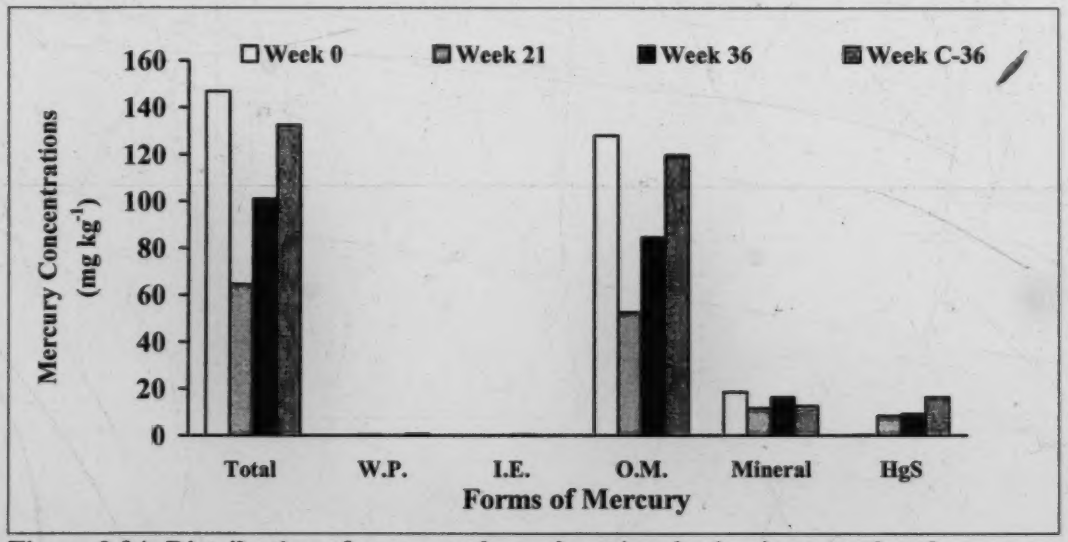

Figure 3.34: Distribution of mercury throughout incubation in control and experimental microcosms.

(W.P.-water-soluble Hg, I.E.-ion exchangeable Hg, O.M.-organic matter associated Hg, mineral –Hg associated with the soil mineral fraction).

4.0 Summary and Implications

4.1 Summary

The present study was intended to determine if mercury in mercury-contaminated soils could be transformed to mercury sulfide, a highly recalcitrant and stable form of mercury. Mercury-contaminated soils were incubated anaerobically for 36-wk with additions of calcium acetate (a soluble carbon and energy source) and calcium sulfate to promote mercury sulfide formation. Various soil and solution analyses completed upon microcosm dismantling provided information about soil mercury and mercury sulfide.

Upon addition to soil, elemental mercury undergoes several transformations, resulting in numerous forms of mercury within the soil. Up to 87% of total mercury within the Turner Valley Gas Plant soil was found as organic matter bound prior to the 36-wk incubation. Because mercury binds strongly to sulfur compounds and S-functional groups within soil organic matter, it is likely that the majority of the organic matter bound mercury is held by stable covalent bonds to sulfur containing sites. Due to its high sulfur content compared to the other organic matter fractions, it is likely that a majority of organic matter bound mercury is found in the humic acid fraction and in the humin fraction.

After incubation, there was a 71% increase in mercury sulfide concentration in both the control and experimental microcosms. However, even with this increase in mercury sulfide only up to 12% in the control microcosms and 9% in the experimental microcosms of total mercury was transformed to mercury sulfide. The majority of total mercury remained as soil organic matter bound in both the control and experimental microcosms after the 36-wk anaerobic incubation. This indicates that mercury

preferentially binds with organic matter in soils and does so strongly. Rates of mercury adsorption onto organic matter are up to 10^5 times greater than desorption rates (Rai et al., 1984). In soils where organic matter is present and the mercury has reverted to other soil bound forms, mainly organic matter bound, conversion of mercury to mercury sulfide does not result in significant changes in the soil mercury distribution. This is because there is very little mercury available in forms able to participate in soil solution chemistry.

4.2 Implications

In aerobic, mercury-contaminated soils with average to high organic matter content it is likely that the majority of soil mercury will be found bound to organic matter. It is unlikely that the once soil mercury has become organic matter bound that it can be transformed to mercury sulfide or any other form of mercury. It required 30% H_2O_2 to dissolve the organic matter and release the organic matter bound mercury. It appears that organic matter-bound mercury is highly stable and can be considered recalcitrant. Not considering mercury toxicity, if the majority of soil mercury is found as organic matter bound it can be considered stable and recalcitrant, thus limiting the environmental threat of mercury through dispersal to air, surface water and ground water.

5.0 References

Abd-el-Malek, Y., and Rizk, S.G. 1963. Bacterial sulfate reduction and the development of alkalinity. II. Laboratory study with soils. Journal of Applied Bacteriology. 26: 14-19.

Adriano, D.C. 1986. Trace Elements in the Terrestrial Environment. Springer-Verlag Inc., New York. pp. 298-328.

Alef, K., and Nannipieri, P. (Ed.) 1995. Methods in Applied Soil Microbiology and biochemistry. Academic Press, New York. pp. 53-54.

Allan C.J., Heyes, A., Roulet, N.T., St Louis, V.L., and Rudd, J.W.M. 2001. Spatial and temporal dynamics of mercury in Precambrian Shield upland runoff. Biogeochemistry. 52:13-40.

Anderson, A. 1979. Mercury in soils. Nriagu, O. (Ed). In: The Biogeochemistry of Mercury in the Environment. Elsevier, North Holland Biomedical Press, Amsterdam, The Netherlands. pp. 79-112.

Barnett, M, Harris, L., Turner, R., Stevenson, R., Henson, T., Melton, R., and Hoffman, D. 1997. Formation of mercuric sulfide in soil. Environmental Science and Technology. 32: 3037-3043.

Benoit, J.M., Mason, R.P., and Gilmour, C.C. 1999. Estimation of mercury-sulfide speciation in sediment pore waters using octanol-water partitioning and implications for availability to methylating bacteria. Environmental Toxicology and Chemistry. 18: 2138-2141.

Benoit, J.M., Gilmour, C.C., and Mason, R.P. 2001. Aspects of bioavailability of mercury for methylation in pure cultures of *Desulfobulbus propionicus* (1pr3). Applied and Environmental Microbiology. 67: 51-58.

Biester, H., and Zimmer, H. 1998. Solubility and changes of mercury binding forms in contaminated soils after immobilization treatment. Environmental Science and Technology. 32: 2755-2762.

Biester, H., Muller, G., and Scholer, H.F. 2002. Binding and mobility of mercury in soils contaminated by emissions from chlor-alkali plants. The Science of the Total Environment. 284: 191-203.

Carter, M.R. (Ed.). 1993. Soil Sampling and Methods of Analysis. Lewis Publishers. Florida. pp. 507.

Clever, H.L., Johnson, S.A., and Derrick, M.E. 1985. The solubility of mercury and some sparingly soluble mercury salts in water and aqueous electrolyte solutions. Journal of Physical Chemistry Reference Data. 14: 601-680.

Cochran, W.G. 1950. Estimation of bacterial densities by means of the "most probably number". Biometrics 6: 105-115.

Conner, J. 1990. Chemical Fixation and Solidification of Hazardous Wastes. Van Nostrand Reinhold, New York. pp. 140-171.

Davis, A., Bloom, N.S., and Que Hee, S.S. 1997. The environmental geochemistry and bio-accessibility of mercury in soils, sediments: a review. Risk Analysis. 17: 557-567.

D'Itri, F.M. 1972. The Environmental Mercury Problem. CRC Press. Cleveland, Ohio.

Dmytriw, R., Mucci, A., Lucotte, M., and Pichet, P. 1995. The partitioning of mercury in the solid components of dry and flooded forest soils and sediments from a hydroelectric reservoir, Quebec (Canada). Water, Air and Soil Pollution. 80: 1099-1103.

Donald, R., and Southam, G. 1999. Low temperature anaerobic bacterial digenesis of ferrous monosulfide to pyrite. Geochimicia et Cosmochimica Acta. 63: 2019-2023.

Dudas, M.J. 1988. Soil Chemistry – Laboratory Manual Soil Science 450. University of Alberta. Edmonton, AB. pp. 52.

Dudas, M.J., and Pawluk, S. 1976. The nature of mercury in Chernozemic and Luvisolic soils in Alberta. Canadian Journal of Soil Science. 56: 413-423.

Dyrssen, D., and Wedborg, M. 1989. The state of dissolved trace sulfide in seawater. Marine Chemistry. 26: 289-293.

Dyrssen, D., and Wedborg, M. 1991. The sulfur – mercury (II) system in natural waters. Water, Air and Soil Pollution. 56: 507-519.

Eganhouse, R.P., Young, D.R., and Johnson, J.N. 1978. Geochemistry of mercury in Palos Verdes sediments. Environmental Science and Technology. 12: 1151-1157.

Erlich, H.L. 1981. Geomicrobiology. Marcel Dekker Incorporated, New York, USA. pp. 157-164.

Fedorak, P.M., Semple, K.M., and Westlake, D.W.S. 1987. A statistical comparison of two culturing methods for enumerating sulfate reducing bacteria. Journal of Microbiological Methods. 7: 19-27.

Gilmour, C.C., and Henry, E.A. 1991. Mercury methylation in aquatic systems affected by acid deposition. Environmental Pollution. 71: 131-169.

Gilmour, C.C., Henry, E.A., and Mitchell, R. 1992. Sulfate stimulation of mercury methylation in freshwater sediments. Environmental Science and Technology. 26: 2281-2287.

Greenberg, A. (Ed). 1985. Standard Methods for the Examination of Water and Wastewater 16th Edition. American Public Health Association, Washington D.C.

Hahne, H.C.H., and Kroontje, W. 1973. The simultaneous effect of pH and chloride concentration upon mercury (II) as a pollutant. Soil Science Society of America Proceedings. 37: 838-843.

Harju, J.A., Kuhnel, V., Charlton, D.S., and Evans, J.M. 1995. Field bases research on elemental mercury spills. Water, Air and Soil Pollution. 80: 1191-1197.

Hartgers, W.A., Lopez, J.F., Sinninghe Damste, J.S., Reiss, C., Maxwell, J.R., and Grimalt, J.O. 1997. Sulfur-binding in recent environments: II. Speciation of sulfur and iron and implications for the occurrence of organo-sulfur compounds. . Geochimicia et Cosmochimica Acta. 61: 4769-4788.

Hempel, M., Wilken, R.D., Miess, R., Hertwich, J., and Beyer, K. 1995. Mercury contaminated sites – behaviour of mercury and its species in lysimeter experiments. Water, Air and Soil Pollution. 80: 1089-1098.

Hogg, T.J., Stewart, W.B., and Bettany, J.R. 1978. Influence of the chemical form of mercury on its adsorption and ability to leach through soils. Journal of Environmental Quality. 7: 440-445.

Holowenko, F.M., MacKinnon, M.D., and Fedorak, P.M. 2000. Methanogens and sulfate-reducing bacteria in oil sands fine tailing wastes. Canadian Journal of Microbiology. 46: 927-937.

John, M.K. 1972. Cadmium adsorption maxima of soils as measured by the Langmuir isotherm. Canadian Journal of Soil Science. 52: 343-350.

Jonasson, I.R., and Boyle, R.W. 1971. Geochemistry of mercury. In: Mercury in Man's Environment. Proceedings of the Royal Society Symposium, Ottawa, Ontario, Canada. February 15-16, 1971. Available: Geological Survey of Canada, Department of Energy, Mines and Resources, Ottawa, Ontario, Canada. pp.

Kaiser, G., and Tolg, G. 1980. Mercury. Hutzinger, O. (Ed). In: Handbook of Environmental Chemistry: Anthropogenic Compounds. Springer-Verlag, Berlin, Germany. pp. 1-58.

King, J.K., Kostka, J.E., Frischer, M.E., and Saunders, F.M. 2000. Sulfate-reducing bacteria methylate mercury at variable rates in pure culture and in marine sediments. Applied and Environmental Microbiology. 66: 2430-2437.

King, J.K., Harmon, S.M., Fu, T.T., and Gladden, J.B. 2002. Mercury removal, methyl mercury formation, and sulfate-reducing bacteria profiles in wetland mesocosms. Chemosphere. 46: 859-870.

Kohut, C., Dudas, M.J., and Luther, S.M. 1995. Investigation of Soil Mercury Distribution at the Turner Valley Gas Plant. Alberta Environmental Protection, Alberta Community Development. Report # HG003-95. pp. 122.
Kohut, C., Dudas, M.J., and Nason, G.E. 2000. Distribution of mercury in soils at a decommissioned gas plant. Canadian Journal of Soil Science. 80: 473-482.

Krauskopf, K.B. 1967. Introduction to Geochemistry. McGraw Hill Book Company, New York. pp. 720.

Landi, S., and Fagioli, F. 1994. The adaptation of the dichromate digestion method for total mercury determination by cold-vapor atomic absorption spectrometry to the analysis of soils, sediments and sludges. Analytic Chimica Acta. 298:363-374.

Lexmond, M., de Haan, F.A.M., and Frissel, M.J. 1976. On the methylation of inorganic mercury and decomposition of organo-mercury compounds-a review. The Netherlands Journal of Agricultural Science. 24: 79-97.

Lindberg, S.E., Kim, K., Meyers, T.P. and Owens, J.G. 1995. Micrometeorological gradient approach for quantifying air/surface exchange of mercury vapours: tests over contaminated soils. Environmental Science and Technology, 29: 126-135.

Lindsay, W.L. 1979. Chemical Equilibria in Soils. John Wiley and Sons. New York. pp. 449.

Lumsdon D.G., Evans, L.J., and Bolton, K.A. 1995. The influence of pH and chloride on the retention of cadmium, lead, mercury, and zinc by soils. Journal of Soil Contamination. 4:137-150.

Melton, J.R., Hoover, W.L., and Howards, P.A. 1971. The determination of mercury in soils by flameless atomic absorption. Soil Science Society of America Proceedings. 35: 850-852.

McGill, W. 1999. Personal Communication. The University of Alberta, Edmonton, Alberta.

Morel, F.M.M., Kraepiel, A.M.L., and Amyot, M. 1998. The chemical cycle and bioaccumulation of mercury. Annual Reviews of Ecological Systems. 29: 543-566.

Nriagu, O. (Ed). 1979. The Biogeochemistry of Mercury in the Environment. Elsevier, North Holland Biomedical Press, Amsterdam, The Netherlands. pp.

Obukhovskaya, T.D. 1982. Mercury sorption by soil minerals. Soviet Soil Science. 14: 49-55.

Oji, L.N. 1998. Mercury disposal via sulfur reactions. Journal of Environmental Engineering. October: 945-952.

Paul, E.A., and Clark, F.E. 1996. Soil Microbiology and Biochemistry. Academic Press. San Diego, California. pp. 340.
Postgate, J.R. 1984. The Sulfate-Reducing Bacteria, 2nd Edition. Cambridge University Press, Cambridge, United Kingdom.

Rai, D., Schmidt, R.A., Schwab, A.P., and Zachara, J.M. 1984. Chemical Attenuation Rates, Coefficients, and Constants in Leachate Migration. Electric Power Research Institute, Inc., Palo Alto, California. pp.

Ramamoorthy, S. and Rust, B.R. 1976. Mercury sorption and desorption characteristics of some Ottawa River sediments. Canadian Journal of Earth Science, 13: 530-536.

Ravichandran, M., Aiken, G.R., Ryan, J., and Reddy, M.M. 1999. Inhibition of precipitation and aggregation of meta-cinnabar (mercuric sulfide) by dissolved organic matter isolated from the Florida Everglades. Environmental Science and Technology. 33: 1418-1423.

Renneberg, A. 2000. Form and removal of mercury from soil. Master's Thesis. University of Alberta. Edmonton, Alberta.

Renneberg, A. and Dudas, M.J. 2001. Transformations of elemental mercury to inorganic and organic forms in mercury and hydrocarbon co-contaminated soils. Chemosphere. 45: 1103-1109.

Revis, N.W., Osborne, T.R., Holdsworth, G., and Hadden, C. 1989a. Distribution of mercury species in soil from a mercury contaminated site. Water, Air and Soil Pollution. 45: 105-113.

Revis, N.W., Osborne, T.R., Sedgley, D., and King, A. 1989b. Quantitative method for determining the concentrations of mercury(II) sulfide in soils and sediments. Analyst. 114: 823-825.

Revis, N.W., Elmore, J., Edenborn, H., Osborne, T., Holdsworth, G., Hadden, C., and King, A. 1991. Immobilization of mercury and other heavy metals in soils, sediment sludge, and water by sulfate reducing bacteria. Biological Processes, Volume 3, Innovative Hazardous Waste Treatment Technology Series. Technomic Publishing Co, Incorporated. Lancaster, PA.

Rogers, R.D. and McFarlane, J.C. 1978. Factors Influencing the Volatilization of Mercury From Soil. U.S. Environmental Protection Agency, Office of Research and Development, Environmental Monitoring and Support Laboratory, Las Vegas, Nevada.

Salloum, M.J., Dudas, M.J., and Fedorak, P.M. 2002. Microbial reduction of amended sulfate in anaerobic mature fine tailings from oil sand. Waste Management Research. 20: 162-171.

Scheelar, M. 1975. Detailed soil survey of the Black Diamond-Turner Valley area. Alberta Institute of Pedology. Report M-75-8.

Schuster, E. 1991. The behaviour of mercury in the soil with special emphasis of complexation and adsorption processes – a review of the literature. Water, Air and Soil Pollution. 56: 667-680.

Semu, E, Singh, B.R., and Selmer-Olsen, A.R. 1986. Adsorption of mercury compounds by tropical soils. Water, Air and Soil Pollution. 27: 19-27.

Siegel, F.R. 1974. Applied Geochemistry. John Wiley and Sons, New York. pp. 77-79.

Sposito, G. 1989. The Chemistry of Soils. Oxford University Press, New York. pp. 277.

St. Louis, V.L., Rudd, J.W.M., Kelly, C.A., Beaty, K.G., Flett, R.J., and Roulet. N.T. 1996. Production and loss of methyl mercury and loss of total mercury from Boreal forest catchments containing different types of wetlands. Environmental Science and Technology. 30: 2719-2729.

Steinnes, E., and Salbu, B. 1995. Trace Elements in Natural Waters. CRC Press, Boca Raton, Florida. pp. 302.

Stewart, W.B., and Bettany, J.R. 1982. Methods of soil analysis part 2: Chemical and Microbiological Properties. ASA-SSSA. Madison, Wisconsin.

Thornton, I. 1983. Applied Environmental Geochemistry. Academic Press, London, England.

Wallschlager, D., Desai, M.V.M., Spengler, M., and Wilken, R.D. 1998. Heavy metals in the environment. Journal of Environmental Quality. 27: 1034-1044.

Wang, J.S., Huang, P.M., Liaw, W.K., and Hammer, U.T. 1991. Kinetics of the desorption of mercury from selected freshwater sediments as infuence by chloride. Water, Air and Soil Pollution. 56: 533-542

Wang, W. 1995. Patterns of total mercury in Onondage Lake, New York. Environmental Science and Technology. 29: 2261-2266.

Willett, K.L., Turner, R.R., and Beauchamp, J.J. 1992. Effect of chemical form of mercury on the performance of dosed soils in standard leaching protocols: EP and TCLP. Journal of Hazardous Waste and Hazardous Materials. 9: 275-288.

Windmoller, C.C., Wilken, R.D., and Jardin, W.D.F. 1996. Mercury speciation in contaminated soils by thermal release analysis. Water, Air, and Soil Pollution. 89: 399-416.

Wren, C.D., and Farrell, C.W. 1995. Mercury in the natural gas industry in Canada. Water, Air and Soil Pollution. 80: 1203-1206.

Yin, Y., Allen, H., and Huang, C. 1997. Kinetics of mercury (II) adsorption and desoprtion on soil. Environmental Science and Technology. 31: 496-503.

Yin, Y., Allen, H., Huang, C., and Saunders, P. 1996. Heavy metals in the environment. Journal of Environmental Quality. 25: 837- 844.

Appendix 1

Physical and Chemical Characteristics of Mercury (Nriagu, 1979).

Melting Point: -38.89 °C
Boiling Point: 357.25 °C
Density: 13.5 g cm^{-3} (at 20°C)
Surface Tension: 480 dynes cm^{-1} (at 20°C)
Saturated Vapor Pressure: 14 mg m^{-3} (at 20°C)

Solubility in Water (Hahne and Kroontje, 1979)

Hg: < 4 μg L^{-1}
HgS: 10 μg L^{-1}

Appendix 2

Order of Utilization of Major Electron Acceptors in Soil (Sposito, 1989).

Reaction	Eh (mV) at pH 7	Measured Redox Potential in Soils (mV)
O_2 Disappearance $\frac{1}{2} O_2 + 2e^- + 2H^+ = H_2O$	820	600 to 400
NO_3^- Disappearance $NO_3^- + 2e^- + 2H^+ = NO_2^- + H_2O$	540	500 to 200
Mn^{2+} Formation $MnO_2 + 2e^- + 4H^+ = Mn^{2+} + 2H_2O$	400	400 to 200
Fe^{2+} Formation $FeOOH + e^- + 3H^+ = Fe^{2+} + 2H_2O$	170	300 to 100
S^{2-} Formation $SO_4^{2-} + 6e^- + 9H^+ = HS^- + 4H_2O$	–160	0 to –150
H_2 Formation $H^+ + e^- = \frac{1}{2} H_2$	–140	–150 to –220
CH_4 Formation $(CH_2O)_n = n/2CO_2 + n/2\ CH_4$	—	–150 to –220

Appendix 3

pe-pH Diagram of Sulfide Species